

A Parametric Design Map Based Approach to Gearing Design

By: Luis Fernandez

Supervisor: Dr. D. Tesar

The University of Texas at Austin

Mechanical Engineering

Fall 2017

Technical Formulation for Performance Measures

Introduction

It is common practice to approach the gear mesh design process by starting out with a needed gear teeth count and/or needed gear dimensions (diameter and/or width). From here, some designers may go directly to online vendor's databases to see if they can find what they have in mind or something that is relatively close. Then, some may look at, and do various calculations on, material properties, stresses, stress modification factors, durability, efficiencies, and dynamics for the gear(s) selected – if these meet certain pre-established criteria of the project at hand, that gear set may be used. Others may go further and conduct Finite Element Method (FEM) analysis or other simulations on their gear mesh. All of these calculations and simulations are valuable and will be needed at some later stage of the gear box design process. However, what this document wants to show is that perhaps a better initial approach of designing gears is to look at parametric design maps. This approach is meant to complement engineering insight in the gear mesh design process, rather than replace it.

In this document, different qualifications are analyzed for a single pair of gears in mesh. The text starts with a definition of the many variables that will be used throughout, as well as bounding of parameters for which parametrical design maps will be made. This is followed by a quick review of diametral pitch, mainly to highlight its geometric importance. Then a section on contact ratio is included; it is an important factor when considering load distribution between gear teeth and dynamic behavior. Afterwards, a section on AGMA bending and contact stress numbers is included due to its popularity in initial design to gauge a gear's performance. This is followed by a section on spur gear efficiency due to rolling losses. Then, a look into spur gear tooth torsional stiffness is given, due to its importance in dynamic behavior prediction and load distribution. Finally, friction torques in spur gears is considered. Each of these sections qualifying gear mesh performs include one or more parametric design map.

There exists many types of gear geometries and gear's teeth shape, the focus of this document is on spur and helical gears with standard involute profile (zero profile shift). Though the parametric design maps in this text are bounded by values in Section 1, it should be noted that the techniques used here can be used for any design parameter ranges.

Section 1: Variables and Design Bounds

1.1 Gearing Variables

Gear Mesh

- g_1 : Driving Gear (its parameters will have subscript 1)
- g_2 : Driven Gear (its parameters will have subscript 2)

Gear Geometry

- N : Number of Teeth
- D : Pitch Diameter
- D_b : Base Diameter
- D_o : Outside Diameter
- R : Pitch Radius
- R_b : Base Radius
- R_o : Outside Radius

Gear Mesh Geometry

- G : Gear Ratio = $D_2/D_1 = N_2/N_1$
- W : Face Width
- P_d : Diametral Pitch
- C or a_x : Center Distance
- β : Helical Angle
- α or α_i : Pressure or Radial (transverse) Angle
- α_{wt} : Working Pressure Angle

Contact and Approach

- m_p : Spur Gear Contact Ratio
- ε_T : Total Helical Contact Ratio
- $\varepsilon_{\text{trans}}$: Transverse Contact Ratio
- $\varepsilon_{\text{axial}}$: Axial Contact Ratio
- H_S : Specific Sliding at Start of Approach Action
- H_T : Specific Sliding at End of Recess Action

Loading

- F_t : Tangential Load
- J : Geometric Tooth Bending Factor
- I : Geometric Tooth Contact Factor
- C_p : elastic coefficient
- s_i : Bending Stress
- s_c : Contact (Pitting) Stress

Bending, Stiffness, and Efficiency

- l_s : Percent Sliding Loss
- f : Coefficient of Friction
- K_s : Gear Tooth Bending Stiffness
- E : Young's Modulus

1.2 Broad Design Bounds

This document is meant to serve as a generic approach to the initial steps of designing a gear train, and as a compilation of some general design trends. For this reason, its focus is on a pair of gears meshing only. Gear design is covered by a wide range of industries, from large systems in wind-turbines and ships, to small systems in cars or hand-held drills. It is difficult to cover all of these design constraints in a single document, which is why the selected bounds below were chosen. They nevertheless do cover a fairly wide range of designs. Some parameters have been fixed, while others will be used in discrete sets, and others will cover by ranges. Not every parameter will be used in every section; this will be clarified per section. Although some continuous ranges are used, single values can be picked-off if needed for a given design.

Fixed

- D_1 : Driving Gear Pitch Diameter: 10"

Sets

- β : Helical Angle: 5°, 15°, 30°
- α or α_i : Pressure Angle: 20°, 25°
- f : Coefficient of Friction: 0.01, 0.05, 0.1

Ranges

- D_2 : Driven Gear Pitch Diameter
 - o Velocity Amplification range: [2", 10"]
 - o Torque Amplification range: (10, 50]
- G : Gear Ratio
 - o Velocity Amplification range: [0.2, 1)
 - o Torque Amplification range: (1, 5]
- P_d : Diametral Pitch
 - o Velocity Amplification range: [7, 15]
 - o Torque Amplification range: [2, 10]
- W : Face Width: [1", 5"]

The above choices cover a very large range of gear mesh designs. This is so because this document is not going after a single application, but instead studying trends from a wide range of designs. The choices of gear diameters are within the medium to large range for gears. This was mainly an arbitrary decision so the gear ratios of 1/5 through 5 can be reached.

Limits on diametral pitch were set so that the number of teeth being study, a product of P_d and D , is between 14 and 500. Where 14 or so teeth is seen in smaller gears, like the 2" D_2 gear, and the 500 or so teeth is seen in the larger gears, like the 50" D_2 gear.

The coefficient of friction set first includes a coefficient which is most desirable, 0.01. It also has one that is most expected to be found in gear meshes, 0.05. And one that is a bit high, 0.1, but may be the case due to constraint such as cost or inexperience.

Performance trends that will be discussed in this document are based around combinations of all the parameters presented above. However, not every parameter will be used in every section below. This will be further clarified in each section. Also, note that the two meshing gears here are not described as Pinion (for the small driving gear) and Gear (for the larger driven gear) as is the case in most gear literature. In this document, both torque and velocity amplification is being considered, in which the small gear may be driving or driven.

The reader should be reminded that the main purpose of the parameter ranges given here is to assess the trends of different criteria that will be presented in this text. In a realistic design scenario, the ranges would be much smaller. For this reason, some design combinations from above may seem unnecessary. For example, a gear with a D of 50" and a W of 1" is unlikely, however for the purposes of understanding the design trends, this unusual combination of parameters is acceptable.

Section 2: Brief Review of Diametral Pitch

The diametral pitch is a measurement of density of number of teeth per gear, it is simply defined as follows:

$$\text{Diametral Pitch} = P_d = \frac{\text{Number of Teeth}}{\text{Pitch Diameter}} = \frac{N}{D} \quad \text{Eq. 2.1}$$

where pitch diameter is measured in inches.

The fact that the diametral pitch (P_d) encapsulates the number of teeth (N) in a gear and its pitch diameter (D) can be very useful when setting up parametric design maps. As will be shown in the coming sections, setting an axis to diametral pitch can help a designer balance N and D choices. For example, if a gear requires a fixed N due to a reduction/amplification, strength, or stiffness expected, then changes in the P_d design map axis can be treated as changes in D (because P_d^{-1} is scaled by N). Or, if a gear is geometrically bounded and requires a fixed D , then the P_d axis can be seen as a N axis (because P_d is scaled by D).

Furthermore, diametral pitch can be seen as a base judgement for gear and gear root thickness. These critical parameters can aid in judging expected strength, stiffness, and bending. Although this is not a topic covered in this text, one should be aware that gear root thickness is also critical in deciding root fillet dimensions for a gear, which in turn is responsible for crack propagation and detection. The following table will summarize these arguments, which will further be expanded on and used throughout the text.

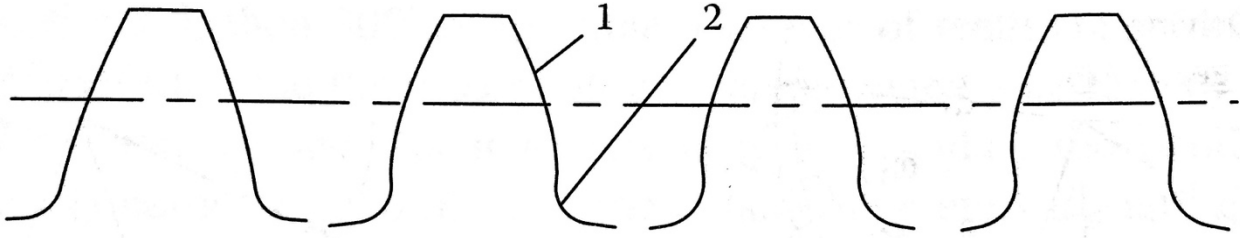
Table 2.1: Diametral Pitch Effects on Gear Teeth Geometry

Hold Fix	Increase	Result	Meaning
Number of Teeth	Diametral Pitch	Decreases Pitch Diameter	<ul style="list-style-type: none"> - In both of these scenarios, by increasing the diametral pitch, the gear teeth become thinner and thus more likely to fail under bending. - Sensitivity for detecting static transmission errors* due to pitting, cracking, or wearing decreases. [13]
Pitch Diameter		Increases Number of Teeth	

* Static transmission error is the rotational deviation of the output gear from its intended position, when a constant torque is applied [13].

Additionally, Figure 2-1 shows the decrease in relative gear root thickness and geometric tooth shape as the diametral pitch is increased.

Figure 2-1: Varying Tooth Root Thickness [6]



When a designer is given or has a needed reduction/amplification ratio or number of teeth per gear or pitch diameters, an increase in diametral pitch (decrease in modulus) may increase the likelihood of the gear mesh teeth failing under bending. One way to reach a higher bending strength can usually be achieved by decreasing the diametral pitch, without changes in diameter or face width [6].

This document is done with English units, therefore diametral pitch instead of modulus is used. It will become clear in this document that for general trends in gearing, diametral pitch is a more significant parameter than pitch diameter or number of teeth individually. This is because diametral pitch encapsulates both of them, and as mentioned in Table 1, a clear trend appears as one increases/decreases it.

Section 3: Contact Ratio

The purpose of this section is to visually provide a designer with general trends that affect the contact ratio, with the hope that the most optimal ratio can be designed for in any problem. The importance of understanding and being able to calculate the contact ratio of meshing gears comes from the fact that by making certain choices in the design process, more gear teeth can carry the transmitted load. Additionally, noise, vibrations, and dynamic load in the mesh can be reduced.

Chapter 7.1 of Klebanov [6] describes the importance of contact ratio while gears are in action. In essence, it is stated that the contact ratio is the proportion of the length of action to the base pitch. For example, if the contact ratio is 2.4, this means that 40% of the time three pair of teeth are in contact and 60% of the time two pair of teeth are in contact. As aforementioned, the more pairs of teeth in contact at any given time, the less load each pair of teeth has to carry. However, one has to be wary of very large contact ratios, as they may increase sliding friction, and cause significant teeth deformation because the teeth are numerous and thin.

Below, equations to find the contact ratio of a Spur and Helical gear mesh are given. This is followed by a Map based parametric study assessing the behavior of the contact ratio. This exercise is intended to advise the reader in making initial choices with respect to the contact ratio.

3.1 Contact Ratio for Spur Gears

The equations to get the contact ratio, m_p , are given below. These all come from [4]. Here the equations are shown in their metric form, directly from the technical paper. The parameter bounds introduced in Section 2 are in English units. In the computer program written to make the designs maps, the English units from Section 2 are first converted to metric units and then the following equations are used.

$$\text{Contact Ratio} \quad m_p = \frac{\sqrt{R_{o1}^2 - R_{b1}^2} + \sqrt{R_{o2}^2 - R_{b2}^2} - C \sin\phi}{m \pi \cos\phi} \quad \text{Eq. 3.1}$$

$$\text{Outside radius} \quad R_o = \frac{1}{2}(D_o) = \frac{1}{2}(D + 2m) = \frac{1}{2}m(N + 2) \quad \text{Eq. 3.2}$$

$$\text{Base Radius} \quad R_b = \frac{1}{2}(D_b) = \frac{1}{2}(D \cos \alpha) \quad \text{Eq. 3.3}$$

$$\text{Pitch Diameter} \quad D = mN \quad \text{Eq. 3.4}$$

Center Distance

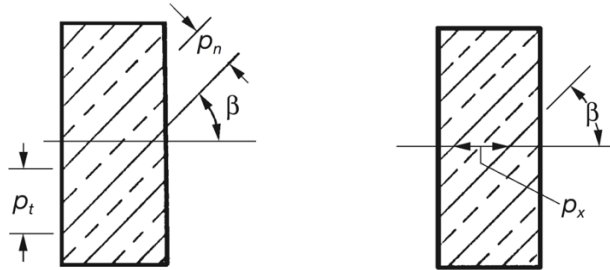
$$C = \frac{m(N_1 + N_2)}{2} = \frac{D_1 + D_2}{2} \quad Eq. 3.5$$

3.2 Contact Ratio for Helical Gears

For Helical gears, the equation for the contact ratio is more involved, and requires the use of the involute equation and inverse involute equation. Due to the high number of computations that will be done, a lookup table cannot be used to deal with the involute equation, thus Appendix A1 shows how to deal with this in an efficient computational formulation.

The contact ratio for a helical gear mesh is the summation of the contact ratio as seen in the transverse (or radial, or circular) direction and the axial direction. Note that for spur gears, one only deals with the contact ratio in the radial direction. Figure 3-1 further clarifies this by showing the direction of the transverse pitch p_t , and the axial pitch p_x . These are the same directions as that of contact for transverse and axial.

Figure 3-1: Transverse p_t and Axial p_x Directional Pitch [4]



Like for the spur gear, these equations also come from [4], and the parameters from Section 1 are converted to metric units before making design maps.

Total Contact Ratio

$$\varepsilon_{total} = \varepsilon_\tau = \varepsilon_{trans} + \varepsilon_{axial} = \varepsilon_\alpha + \varepsilon_\beta \quad Eq. 3.6$$

Radial Contact Ratio

$$\varepsilon_\alpha = \frac{\sqrt{\left(\frac{d_{o1}}{2}\right)^2 - \left(\frac{d_{b1}}{2}\right)^2} + \sqrt{\left(\frac{d_{o2}}{2}\right)^2 - \left(\frac{d_{b2}}{2}\right)^2} - a_x \sin\alpha_{wt}}{\pi m_t \cos\alpha_t} \quad Eq. 3.7$$

Axial Contact Ratio

$$\varepsilon_\beta = \frac{W \sin\beta}{\pi m_n} \quad Eq. 3.8$$

Outer Diameter

$$d_a = d + 2h_a \quad Eq. 3.9$$

Base Diameter

$$d_b = d \cos\alpha_t \quad Eq. 3.10$$

Center Distance

$$a_x = \left(\frac{N_1 + N_2}{2} + y \right) m_t \quad Eq. 3.11$$

Center Distance Increment Factor

$$y = \frac{Z_1 + Z_2}{2} \left(\frac{\cos\alpha_t}{\cos\alpha_{wt}} - 1 \right) \quad Eq. 3.12$$

Working Pressure Angle

$$\operatorname{inv} \alpha_{wt} = 2 \tan\alpha_t \left(\frac{x_{t1} + x_{t2}}{z_1 + z_2} \right) + \operatorname{inv} \alpha_t \quad Eq. 3.13$$

$$\text{or } \alpha_{wt} = \cos^{-1} \left(\frac{d_{b1} + d_{b2}}{2a_x} \right) \quad Eq. 3.13.a$$

Normal Module

$$m_n = m_t \cos\beta \quad Eq. 3.14$$

$$\text{Addendum} \quad h_a = (1 + y - x_{t2})m_t = (1 + y - x_{t2})m_t \quad \text{Eq. 3.15}$$

$$\begin{aligned} \text{Pitch Diameter} &= m_t N & d \\ & \qquad \qquad \qquad \square q. 3.16 \end{aligned}$$

Above, two equations are given for the working pressure angle. Eq. 3.13 is used to initially calculate this angle, while Eq. 3.13.a can be used to check the value after the center distance is found. Note that if no profile change ($x_t = 0$) nor center distance increment ($y = 0$) is added, then the meshing gears are standard, with no changes in addendum. The profile change is included here for future reference. For succinctness, no profile change will be included in the design maps below.

3.3 Parametric Study

In this section, meaningful graphical maps are extracted from the equations above. From this, a designer will be able to get a feel for the sensitivity of the contact ratio to certain parameters. Furthermore, different design trends can be seen, and design decisions made, as one moves around the map. These cannot be easily understood by just looking at the equations.

3.3.1 Spur Gear Mesh

When mapping the contact ratio for a spur gear there are few choices to set as the map base axis. To get a physical sense of the gear size and also be able to quickly get number of teeth per gear or the gear ratio, diametral pitch and pitch diameter of the driven gear are set as the base axis. The design maps are separated into velocity and torque amplification; the design bounds defined in Section 2 are used. In each map, results for 20° and 25° pressure angles are shown.

Figure 3-2: Contact Ratio for Spur Gear Mesh, Velocity Amplification

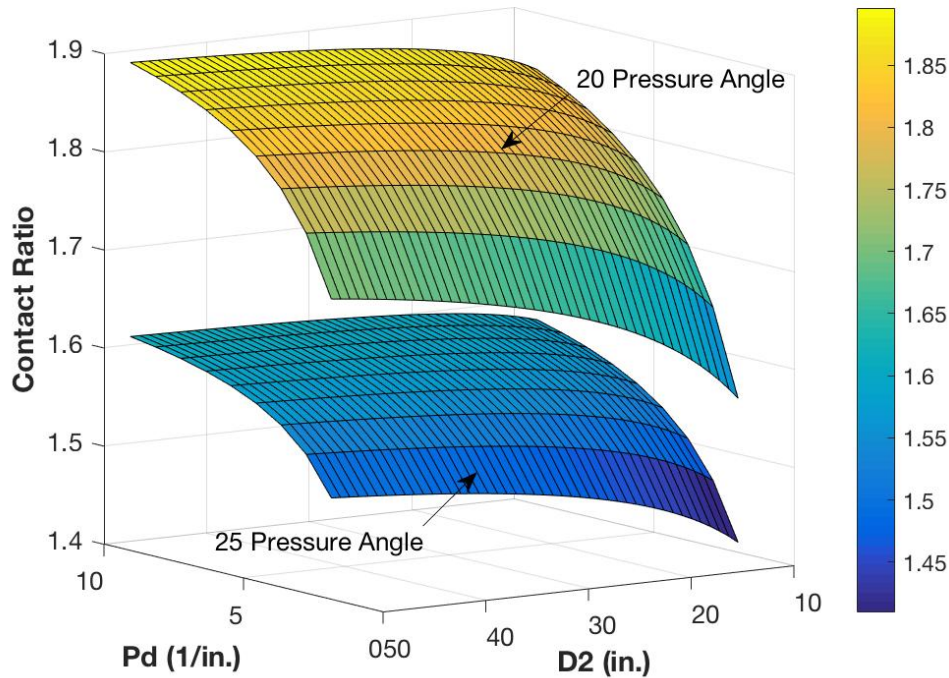
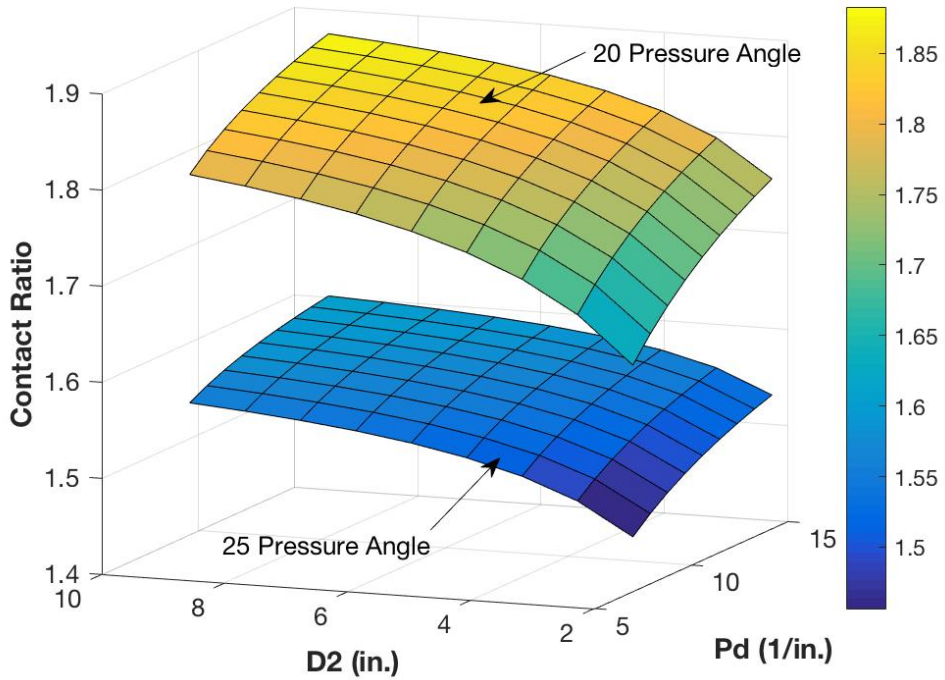


Figure 3-3: Contact Ratio for Spur Gear Mesh, Torque Amplification



From these maps alone, a lot of information can be extracted. If a number in the range of P_d is multiplied with a number in the range of D_2 , then the number of teeth in the driven gear is known. If it is multiplied by the fixed D_1 , the teeth count for the driver gear is known. If any D_2 is divided by fixed D_1 , then the ratio, whether velocity or torque amplification, is known. And, for any of these parameters that one may be looking at, the contact ratio for 20° and 25° pressure angle can be evaluated,

Figure 3-2 and 3-3 show that the contact ratio is greater for a smaller pressure angle. But the difference is not great, as for both graphs, the difference is about 15%. It is also clear that increasing P_d or D_2 will increase the contact ratio as well. If any D_2 value, or for the fixed D_1 value, is considered as P_d increases, the number of gear teeth for either will increase – i.e. more teeth, the higher the contact ratio. Also, for any diametral pitch, as the gear ratio increases, so does the contact ratio.

The shape of the design maps shows that contact ratio number for a spur gear has about the same sensitivity for D_2 as it does for P_d . Due to the design bounds set in Section 2, instead of D_2 , that axis could be covered by gear ratio. Nevertheless, the trends highlighted in the previous paragraph would be observed as well.

It's worth mentioning that power losses for a velocity amplifier, or when back-driving a gear train, is lower when the reduction ratio is lower [12]. Therefore, for these systems, the benefit of a larger contact ratio (due to a large G) needs to be weighed against the expected larger power loss.

Overall, spur gears typically have low contact ratios, unless changes in addendum height or profile shifts are applied. Next, helical gears are considered, and it is clear that these gears have higher contact ratios due to their helical angle over a range of gear face widths

3.3.2 Helical Gear Mesh

As was done for the spur gears, a map of contact ratio with base axis of D_2 and P_d was created. This design map is included in Appendix A2, Figure A2-1. This map is not part of the main text because it shows that for helical gears, the sensitivity of the contact ratio to D_2 is virtually unimportant. Whenever this is the case, a 3D map is not as valuable as when non-linear relationships are present. If D_2 was replaced by G , the same linearity would be seen.

A clear factor that will affect contact ratio for a helical gear, besides its helical angle, is its face width. For this reason, the base axes have been chosen to be diametral pitch and face width. Because P_d and W have no relationship with gear ratio, there is no need to have two separate design maps for velocity and torque amplification.

In every figure below, a transparent horizontal plane is set at contact ratio of 4. This is done as a hint to the designer to keep in mind that as one goes to higher contact ratios (higher than 4 or so), problems with contact properties

may arise. That is, due to machining inaccuracies, deformation, and other factors, not all teeth of gears involved in the contact ratio may be engaging fully, causing failures as if the gear mesh had a lower contact ratio.

Figure 3-4: Contact Ratio for Helical Gear Mesh, 20° Pressure Angle

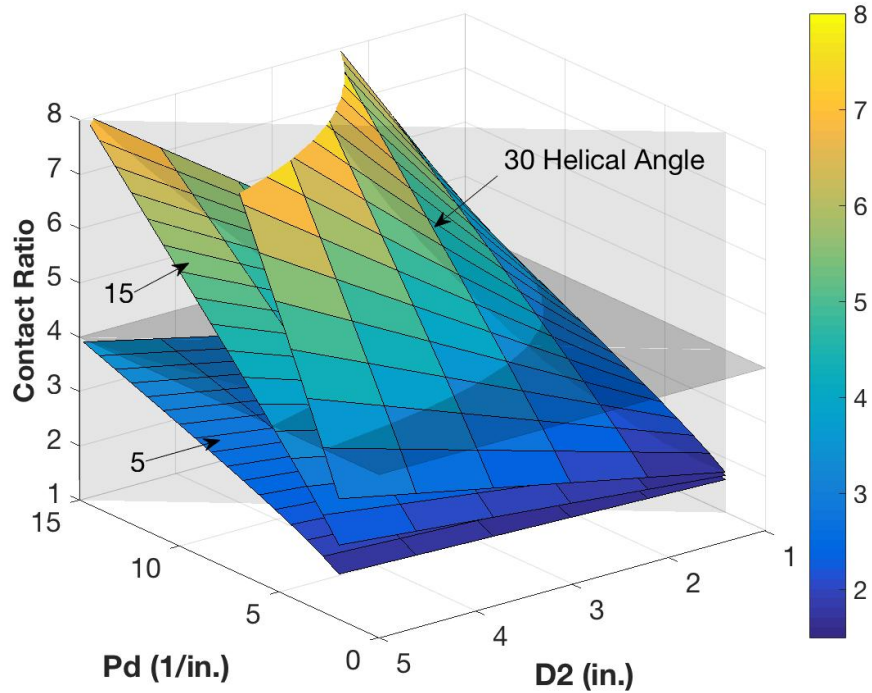
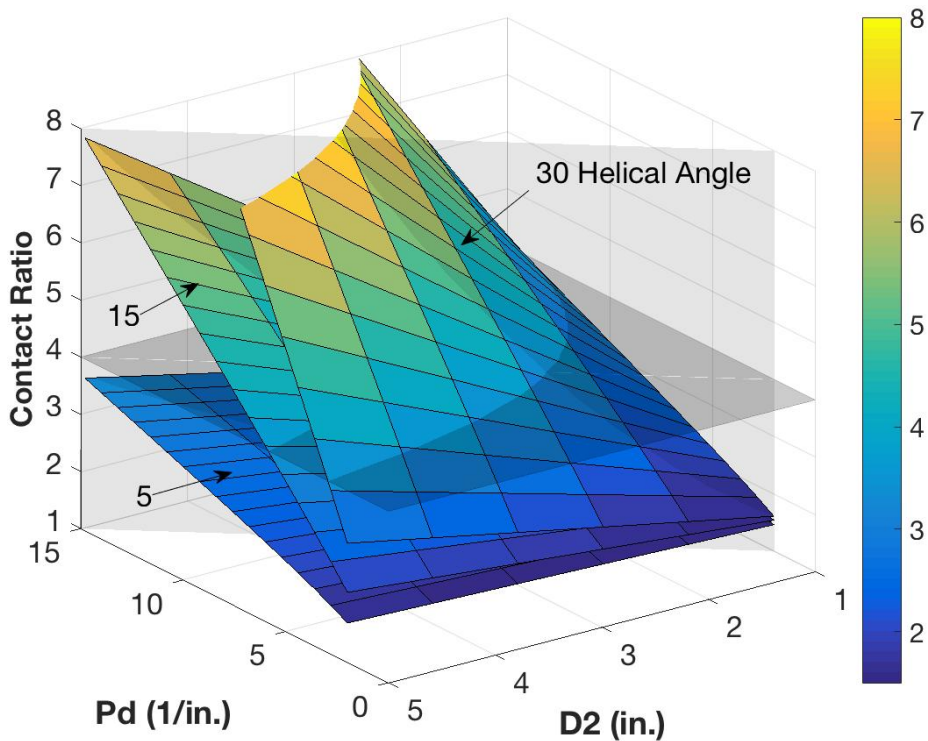


Figure 3-5: Contact Ratio for Helical Gear Mesh, 25° Pressure Angle



After the maps were created, it became clear that the maximum contact ratio for any combination of P_d and W is at or near the diagonal plane defined by the following equation:

$$W = \frac{4}{13}P_d + \frac{5}{13} \quad Eq. 3.17$$

As was the case for the spur gears, the 20° pressure angle reaches slightly higher contact ratios than the 25° . This difference is so small that it may be negligible. Although, at a higher pressure angle, the gear's thicker base gives it higher bending-load-carrying capacity. This decrease in contact ratio results in the teeth generating more operating noise [3].

Both maps above show the same trend for diametral pitch as spur gears do, as P_d increases so does contact ratio. This can also be seen as if given a fixed D_2 , or using the fixed D_1 , more teeth will increase contact ratio. Or, if given a fixed number of teeth, a smaller diametral pitch would lead to higher contact ratios – i.e. teeth would be closer together and the helical angle would cause more of them to be in contact at any given time.

Not only does increasing W increase contact ratio, it also increases the sensitivity that P_d has on the contact ratio. That is, for higher W , slight increases in P_d produce larger increases in contact ratio than smaller W . One can conclude then, that if the W is not much of a concern, then one can use a smaller pitch diameter, or a larger W to be able to reach higher contact ratios.

As expected, increasing the helical angle increases the contact ratio. What one should note however is that the sensitivity of the contact ratio to the helical angle increases as P_d and/or W increase. As the helical angle decreases, the design map becomes flatter. This is because at low helical angles, the gear, and therefore the map, will resemble a spur gear.

Section 4: AGMA Bending and Contact Stress

When doing gear refinement work at the end of a design cycle, great care should be taken at selecting various needed stress correction factors (k values) that will alter the bending and contact stress of a gear mesh. In this document, a holistic view is sought that is more aligned with the geometry of the meshing gears than with the stress coefficient factors that are, for the main part, dependent on material, velocities, manufacturing, and duty cycle. For this reason, every k value is set equal to 1, and the stress numbers are elementary formulations as follows [3]:

$$Bending Stress: \quad s_t = \frac{F_t P_d}{WJ} \quad Eq. 4.1$$

$$Contact Stress: \quad s_c = C_p \sqrt{\frac{F_t}{D_s W I}} \quad Eq. 4.2$$

Where D_s is the pitch diameter of the smaller gear in mesh. C_p has been set to 2300 psi for steel-on-steel meshing [15].

To reduce complexity and to focus mainly on the variation of the stresses, the equations above will be given a unit tangential load value of 1,000 lb. Approximate I and J values are assumed as shown in the table below, and explained in Appendix B.

Table 4.1: Average I and J Values

Pressure Angle (α)	Helical Angle (β)	Average Geometric Tooth Stress Factor	
		Bending (J)	Contact (I)
20°	5°	0.38	0.14
	15°	0.52	0.17
	30°	0.46	0.18
25°	5°	0.59	0.14
	15°	0.6	0.18
	30°	0.55	0.18

By taking the averages this way, as explained in Appendix B, I and J become dependent on pressure and helical angles only.

4.1 Parametric Study of AGMA Bending Stress

4.1.1 Parametric Design Maps

For this section, Equation 4.1 is used alongside the above mentioned values of J and the tangential load F_t . Below, bending stress is plotted against the range of values for the face width and diametral pitch, as defined Section 1. The first map is for gear meshes with a 20° pressure angle, the second with a 25° pressure angle. Each map has surfaces for 5° , 15° , and 30° helical angles. These figures apply to both torque and velocity amplification.

Figure 4-1: Bending Stress for 20° Pressure Angle Gear Meshes

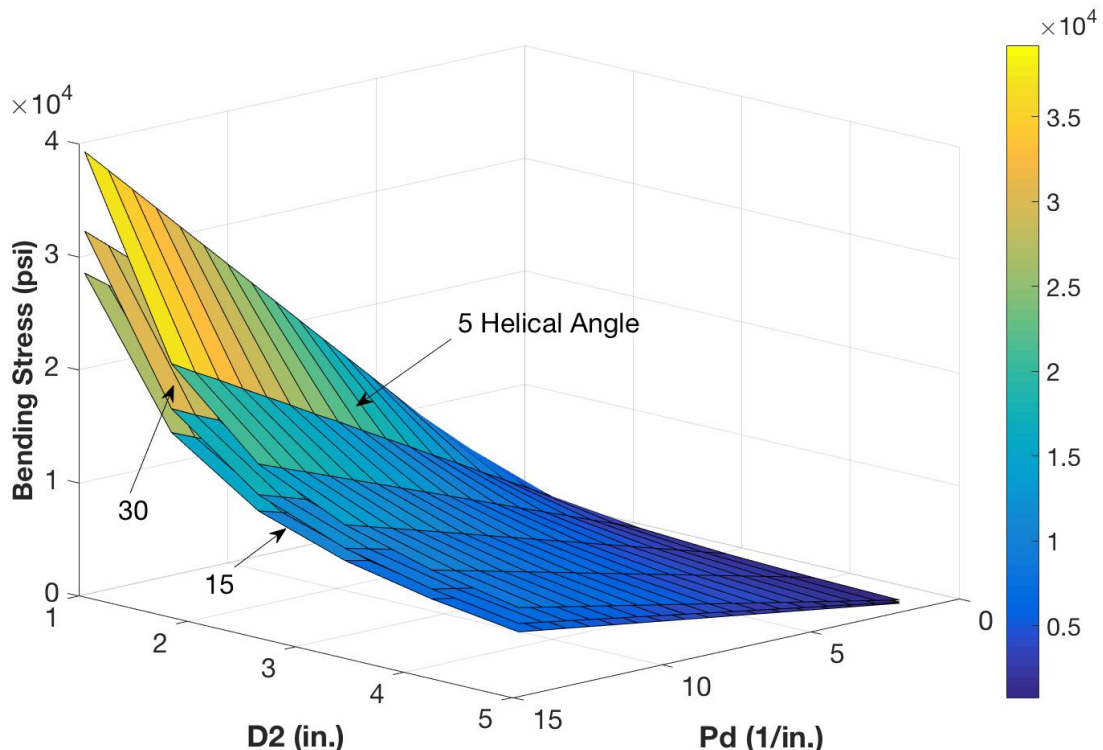
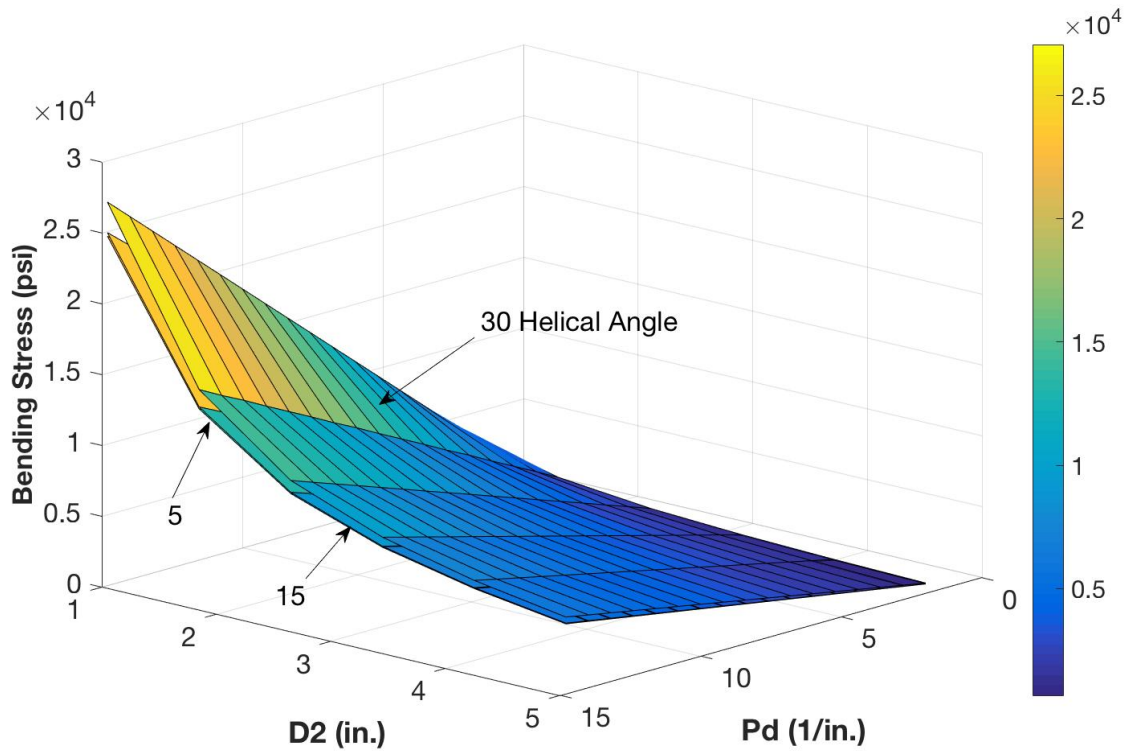


Figure 4-2: Bending Stress for 25° Pressure Angle Gear Meshes



4.1.2 Maps' Sensitivity to Parameters

Both figures above show that at large face widths and/or low diametral pitch, the values of bending stress numbers start converging into each other, regardless of helical angle. This means that if the pitch diameter is held fixed, as the number of teeth for the driving or driven gear decreases, changing the helical angle has a smaller and smaller effect on the bending stress number.

The same can be said about the face width, without having to hold anything fixed. That is, as the face width increases, regardless of diametral pitch, the trend is that the helical angle will have a smaller effect on the bending stress number. Of course, the effects of the helical angle become even smaller as the diametral pitch decreases. In application, this trend will be limited by geometric space constraints of the gearing system.

4.1.3 Maps' Trends of Parameters

The decrease in bending stress due to a decrease in diametral pitch can be studied by looking at the behavior of the number of teeth or the pitch diameter.

If the pitch diameter is held fixed for the smaller gear in a gear mesh, as the diametral pitch decreases, the number of teeth will also decrease. This leads to thicker teeth, which are less likely to fail under bending; this can be justified by the lower bending stress numbers. However, if one looks at the contact ratio maps in Section 3 (Figures 3-3 and 3-4), as the diametral pitch decreases, the contact ratio also decreases, meaning that load-sharing between teeth decreases. A decrease in load-sharing, i.e. more load per tooth, should increase bending stress, this is not directly observed in Figure 4-1 and 4-2.

In another case, if the number of teeth in the smaller gear are held constant, as diametral pitch decreases, pitch diameter increases. This will lead to more circumferential space per tooth, thus wider teeth that are able to better resist bending. This is justified by the lower bending stress numbers in the maps above.

As face width of the gear mesh increases, the bending stress values decrease. This can be attributed to the fact that a wider gear tooth has more surface area in which to distribute the transfer loads. Furthermore, if one looks at Figure 3-3 and 3-4, it is clear that an increase face width leads to an increase in contact ratio. That is, due to the distribution of load on multiple teeth, the load per tooth decreases. This is directly observed in Figure 4-1 and 4-2.

Figure 4-1 and 4-2 show no clear trend with respect to helical angle. This is mainly due to the nonlinearity of the geometric bending tooth stress factor (J); these factors come from AGMA [16]. Due to the fact that this

document is not after refinement, for each helical and pressure angle combination, J is calculated as an average (see Appendix B). If J is calculated for every gear mesh being tested, results may be more realistic.

It is worth pointing out that most gearing literature [3] states that at higher pressure angles, the bending load carrying capacity increases. This is seen in the above Figure 4-1 and 4-2. These figures show that a higher pressure angle increases the bending stress load carrying capacity. This is seen by lowered bending stress number when going from the 20° to 25° .

4.2 Parametric Study of AGMA Contact Stress

4.2.1 Parametric Design Maps

These maps will be calculated using Equation 4.2, along with the unit load defined above and the average geometric tooth contact stress factors, I , in Table 4.1. Due to the nature of the equation, and the parameters set in Section 1, the contact stress will be plotted against the pitch diameter of the small gear in the gear mesh, and the face width of the gear mesh. As seen in Table 4.1, the average I values repeat themselves, in reality there is only three distinct I values in that table. For this reason, only two plots will be created, one for the torque amplification and another for the velocity amplification. Each will have the three I values from Table 4.1, which are combinations of pressure and helical angles.

Notice that, based on the parameters set in Section 1, when working with torque amplification, the pitch diameter of the smaller gear will always be $10''$. For this reason, as seen in Figure 4-3, there is no need to have a dedicated axis for the pitch diameter. For velocity amplification, the pitch diameter of the smaller gear in the gear mesh will change, thus Figure 4-4 below does have an axis dedicated to pitch diameter.

Figure 4-3: Contact Stress for 20° and 25° Pressure Angle, Torque Amplifying Gear Meshes

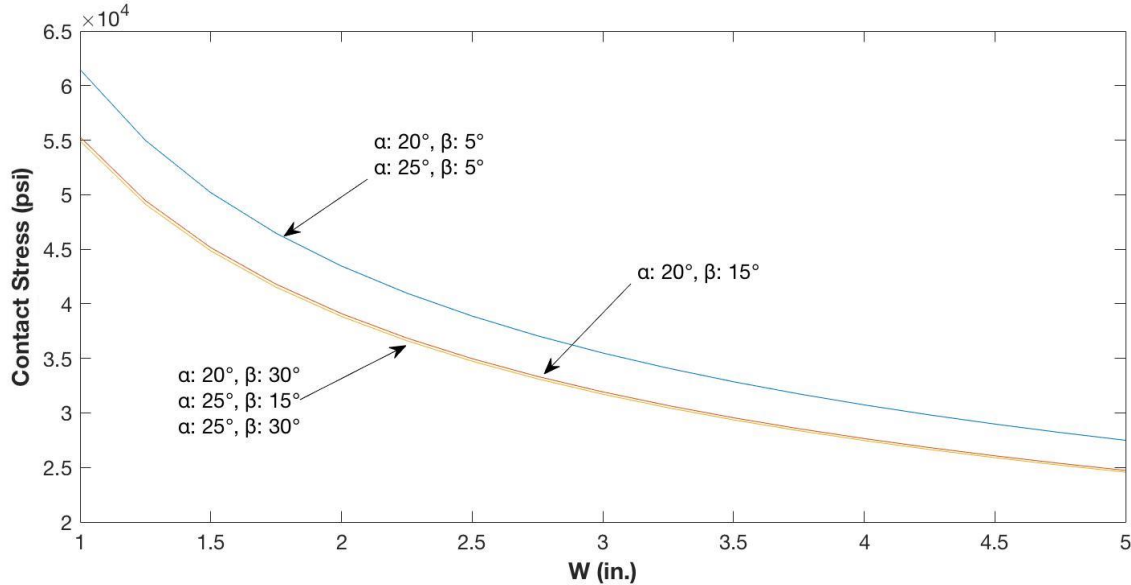
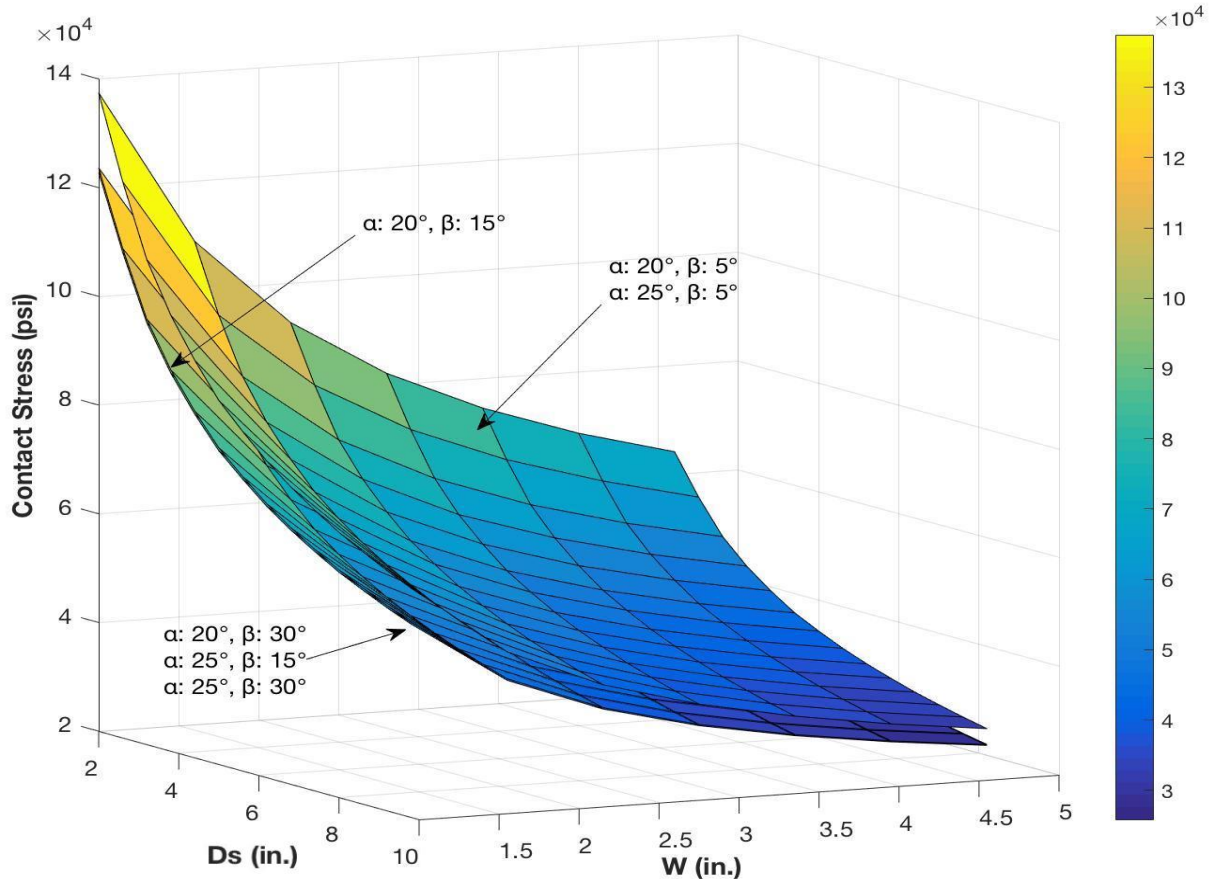


Figure 4-4: Contact Stress for 20° and 25° Pressure Angle, Velocity Amplifying Gear Meshes



4.2.2 Maps' Sensitivity to Parameters

Figure 4-3 can be thought of as a slice of Figure 4-4 with a pitch diameter of 10". For this reason, it can be said that for both velocity and torque amplification, the contact stress number is very sensitive to face width. For velocity amplification alone, it appears that the sensitivity to face width and pitch diameter is fairly similar. For both, it can also be said that the contact stress number has very little sensitivity to pressure angle. This is the case because given any helical angle, a small change in pressure angle (5°) does not change the location of the map/line; i.e. virtually no change in contact stress.

It is difficult to comment on the sensitivity due to the helical angle because for helical angle of 15° and 30°, the plots do not change very much. Unlike the bending stress maps, these maps do not converge into each other, but instead appear to be scales of each other.

The difficulty in gauging the expected contact stresses, based on the helical and pressure angle, is mainly due to the nature of the geometric tooth contact stress factor. Even if it is calculated for every gear mesh, this issue may persist. Overall though, this shows the importance of parametric design maps in gear design. In designing with equations only, this subtlety would likely be overlooked.

4.2.3 Maps' Trends of Parameters

Due to the direct use of the geometric gear parameters, the trends for these maps are more straightforward. The contact stress number is decreased with increases in the pitch diameter of the smaller gear. As mentioned earlier, increasing pitch diameter leads to thicker gear teeth that are able to carry load more effectively. If the number of teeth, N , is fixed, as pitch diameter increases the diametral pitch will decrease. If one looks at Fig. 3-3 and 3-4, the general trend is that decreasing diametral pitch decreases contact ratio. That is, load carried per tooth is higher. which is not directly observed in Figure 4-4.

The maps show, as can be found in the literature [3], that increasing the face width decreases the contact stress level; i.e. the transfer load is being distributed over a large tooth face area. Fig. 3-3 and 3-4 align with this observation, as they show the general trend that as face width increases, contact ratio increases. This decrease in contact stress due to larger face widths, and/or large pitch diameters of the smaller gear, could be used to justify using safety factors (k) that may be less conservative.

Section 5: Tooth Bending Stiffness

5.1 Background on Gear Mesh Stiffness

Taking into account mesh stiffness is important because it helps predict the dynamic behavior of a single gear mesh as part of a gear box system. It also aids in determining the load distribution in an individual tooth as the contact ratio increases to values greater than one [8]. Both [source_Sanchez] and [8] show ways of calculating gear stiffness via derivations of analytical formulas based around the point of contact travel. These also list multiple ways others in the gear literature have approached this problem, and how their methods provide reasonable approximations. Kiekbusch [5] calculates the torsional mesh stiffness of spur gears by finding equations for the stiffness of the gear body, the bending stiffness of the teeth, and the contact stiffness. Each of these stiffness values is summed as stiffnesses in series, a method also seen in [source_Sanchez] and [8]. Each stiffness equation is found via selection of critical parameters and then running Finite Element Analysis (FEA) simulations to fit those parameters into equations.

Kiekbusch [5] points out that FEA models offer the best results when looking at gear mesh stiffness, even with variations in the number of teeth in contact. [8] and [source_Sanchez] both compare their results to FEAs. Due to the manner of derivation, the equations on [5] are relatively simple, as seen below (Eq. 5.1). [8] and [source_Sanchez] have more involved procedures of calculating stiffness, taking into account more parameters in the process. Nevertheless, these papers show mesh stiffness analytical formulations can be comparable to models from FEAs. The benefit then is that computational time can be reduced by working with these equations to analyze a few designs. The benefit that *this* document wants to show is that if these formulations are carefully plotted into parametric design maps, then a novice working in gear design has a new, and relatively easily understood, way to visually gauge gear mesh stiffness in their design choices.

5.2 Equation to Approximate Bending Stiffness in Spur Gears

This document is going to show a first step towards visualizing gear mesh stiffness trends by studying the bending stiffness of a tooth in a single contact spur gear mesh. The formulation that will be used comes from [5], and it is as follows:

$$k_s = CEW \left(\frac{1}{P_d} \right)^2 N^{2.2} \quad Eq. 5.1$$

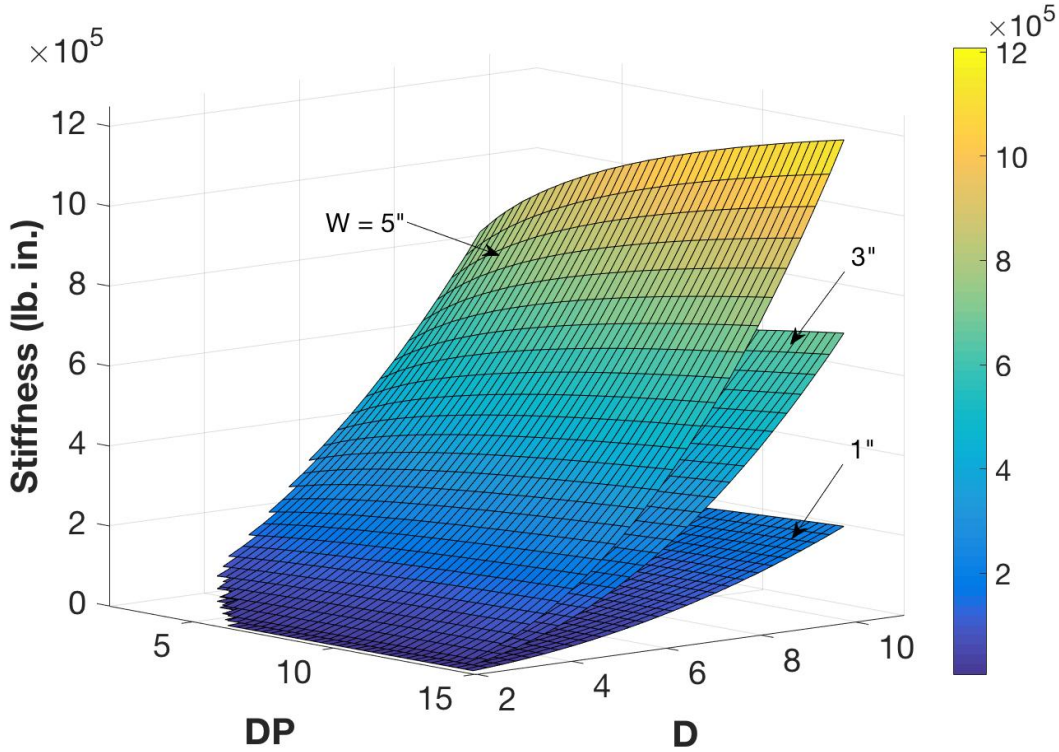
Where K has units of lb.in. C is given to be 0.00032. E is the Young's Modulus of the gear's material – in this section only steel gears are considered (due to their common use), which have E of 29 Mpsi [7]. W is the face width. The discrete values in Section 1 will be used. P_d is the diametral pitch, and the full range defined in Section 1 will be used. N is the number of teeth of the gear of interest.

[5] states that this equation is within 7% from results of an FEA model. The original equation was written for metric units, but is changed here to English units by using the diametral pitch. Eq. 5.1 shows an independence of pressure angle, which is odd because pressure angle has an effect in the thickness of a gear tooth. The author does not even mention the pressure angle used to arrive at these equations. Other sources, [source_Sanchez] and [8], include the pressure angle in their formulation. However, due to the time constraint of the current project, and the fact that this document is just showing the initial steps of what is possible and beneficiary of parametric design maps, the simplicity of Eq. 5.1 is appropriate.

5.3 Bending Stiffness Parametric Design Map for Spur Gears

Failure is most common in the smaller gear, be it the driving or driven gear. Given the parameters being studied, the smaller gear will be either 10" in torque amplification, or from 2" to less than 10" in velocity amplification. For this reason, the map below has its parameter D (pitch diameter), set from 2" to 10".

Figure 5-1: Stiffness as a Function of Diametral Pitch and Pitch Diameter



This map shows that the stiffness of a single tooth increases as the pitch diameter increases. Physically, if the number of teeth are kept constant and the pitch diameter increases, then the thickness of the gear's teeth will increase. This adds to its stiffness by the fact that it involves more material under load.

The stiffness is also seen to increase as the face width increases. This can be attributed to the large contact area which will share the load. As the diametral pitch increases, the stiffness increases slightly. If the pitch diameter is fixed, an increase in diametral pitch means an increase in the number of teeth, which means less space per tooth, i.e. thinner teeth. This is not expected because a thinner tooth (due to having less material) is expected to have a lower stiffness. In [8], even though the pitch diameter is not fixed, it is shown that as number of teeth increases, the stiffness of a single tooth decreases (Fig. 10 (a) and (b) in [8]).

Overall, the parameter with the most influence is the pitch diameter; its influence becomes stronger as face width increases. Also, it can be seen that an increase in face width becomes more significant when the pitch diameter increases, at least more than 4". I.e., if one was designing for a gear that needed to be less than 6" or 4" in pitch diameter, the increase in volume of the gear (and thus the increase in weight/inertia) due to an increase in face width may not be justified. Diametral pitch is the least significant parameter in this map due to its slight increase in stiffness.

It should be noted that the jagged lines at the lower left of the map symbolize the map discarding results which have less than 15 teeth.

5.4 Simple Approximation of Bending Stiffness for Helical Gears Based on Spur Gear Formulation

It appears that a rather simple formula change will give us the approximate torsional stiffness of helical gears. The normal contact force $F_{c,h}$ for helical gears is increased by the $\cos \beta$ value of the spur gear contact force $F_{c,s}$

$$F_{c,h} = \frac{F_{c,s}}{\cos \beta} \quad Eq. 5.2$$

Hence, this force $F_{c,h}$ is increased by the factor $1/\cos \beta$ relative to $F_{c,s}$ such that the stiffness of the helical gear k_h is reduced by $\cos \beta$ relative to the spur gear tooth bending stiffness k_s :

$$k_h = k_s \cos \beta \quad Eq. 5.3$$

5.5 Conclusion

Tooth stiffness in a gear can be difficult to calculate for a novice designer. The non-linear complexity seen in Fig. 5-1, and in [5], [8], [10], can make the task daunting. This is why maps like these can ease any designer into considering stiffness when making initial design decisions. In future work, it is expected that more complex, and hopefully more accurate, calculations can be used to make a map like the ones shown here.

Currently, a source in the gear literature has not been found to compare the results from Fig. 5-1. As explained in the previous subsection, most of the results make sense. However, it is the hope that as this work is continued, that a formulation which has comparable results can be used. Note that the results from the source of Eq. 5.1 cannot be used because the results shown are only for the summation is series of combined stiffnesses of the gear body, the bending stiffness of the teeth, and the contact stiffness.

In this section, only single tooth contact was considered. In reality, spur gears can have higher contact ratios, and helical gears can have even higher contact ratios. Sources 12 through 17 in [8] show formulations for stiffness in higher contact ratios and helical gears. Besides the increase in load distribution due to increase in contact ratio, it can also decrease the required mesh stiffness. However, one should then also consider the dynamic effects of discontinuous mesh stiffness [8] has. As discussed in Section 3, having a contact ratio greater than one means that the gear mesh will fluctuate between actual contact ratios. This also causes fluctuation in mesh stiffness. A closer look at the dynamic response of the system may be considered in more careful future work.

Furthermore, a look at gear mesh stiffness, not just tooth stiffness, may be beneficial, and not too computationally taxing [5]. In general, the total tooth mesh stiffness is obtained by multiplying the single tooth stiffness by the contact ratio.

Section 6: Spur Gear Efficiency Loss Due to Sliding Friction

In this section, Shipley's method as described in *Comparison of Spur Gear Efficiency Methods* will be used. This method only accounts for sliding and windage losses, not rolling losses. However, this method places limitation on windage losses, such that the gear diameter must be less than 20", and that the gear width-to-diameter ratios be approximately 0.5. This does not conform with the parameters studied in this document (parameters presented in Section 1). For this reason, only sliding losses will be considered.

It should be noted that in Shipley's method, the two gears in mesh for which efficiency is being calculated are defined as pinion and gear. Pinion is known to be the smaller gear in the mesh and it drives the gear; the gear is known to be the larger gear in the mesh. Because in this document both torque amplification and velocity amplification are being considered, the driving gear will not always be the smaller gear in the mesh. For this reason, the pinion and gear notation of Shipley's equation will be replaced with the notation being used in this document.

The equations are presented as follows [1]:

$$\text{Spur Gear Percent Sliding Loss} \quad l_s = \frac{50f}{\cos \alpha} \frac{(H_s^2 + H_T^2)}{(H_s + H_T)} \quad \text{Eq. 6.1}$$

$$H_T = \frac{(G + 1)}{G} \left\{ \left(\sqrt{\left(\frac{R_{o1}}{R_1} \right)^2 - \cos^2 \alpha} \right) - \sin \alpha \right\} \quad \text{Eq. 6.2}$$

$$H_s = (G + 1) \left\{ \left(\sqrt{\left(\frac{R_{o2}}{R_2} \right)^2 - \cos^2 \alpha} \right) - \sin \alpha \right\} \quad \text{Eq. 6.3}$$

Where, from the parameters defined in Section 1, outside and pitch diameters will be calculated as follows:

$$R_o = \frac{1}{2} \left(D + \frac{2}{P_d} \right) = R + \frac{1}{P_d} \quad \text{Eq. 6.4}$$

$$R = \frac{D}{2} \quad \text{Eq. 6.5}$$

6.1 Parametric Study of Sliding Loss for Spur Gears

6.1.1 Parametric Design Maps

To follow along with the maps presented for the contact ratio and contact/bending stress sections, these maps will use diametral pitch as one of their axes. Doing so gives a lot of flexibility when discussing the geometry of the gear. For the other axis, the only ranges left, as defined in Section 1, are gear ratio or pitch diameter of the driven gear. To directly get a geometrical understanding of the parameters under consideration, pitch diameter will be used. Plus, the gear ratio can be quickly calculated given the fact that the driven gear has a fixed pitch diameter of 10".

For each coefficient of friction, two maps will be created: one for the velocity amplification parameters and the other for the torque amplification parameters. In each map, results will be shown for pressure angles of 20°, 25°.

While making the parametric maps, it was realized that changing the friction coefficient just scales the map. For this reason, below only maps with coefficient of friction of 0.05 will be shown – they are enough to see the main trends of the equations above. The maps for coefficient of friction of 0.01 and 0.1 will be included in Appendix C, Figure C-1 though C-4.

6.1.2 Maps' Sensitivity to Parameters

The sensitivity of the sliding loss due to pressure angle is very small. This is seen by the fact that in both figures below, the plots for each pressure angle are very close together.

In the torque amplification maps, Figure 6-1, it can be seen that loss is more sensitive to diametral pitch than to pitch diameter of the driven gear. The velocity amplification maps, Figure 6-2, show that sliding loss here is about equally sensitive to diametral pitch and pitch diameter of the driven gear.

6.1.3 Maps' Trends of Parameters

Both maps follow the trend that as diametral pitch and pitch diameter decrease, the percent energy loss also increases. When looking at the torque amplification map, higher losses are seen as the pitch diameter of the driven gear approaches the pitch diameter of the driving gear, that is, 10". In the velocity amplification map, this happens as the pitch diameter of the driven gear becomes smaller and smaller. In both cases, if diametral pitch is fixed and pitch diameter decreases (increasing loss), then the number of teeth are also decreasing. Figure 3-2, Contact Ratio for Spur Gear Mesh, shows the general trend that as pitch diameter of the driven gear decreases, the contact ratio also decreases. Therefore, it can be concluded that this increase in sliding loss is due to decrease in gear tooth count and thusly contact ratio as well.

Although not under consideration in this text, a note should be made about backdrivability and the velocity amplification map. A great deal of power transmission has the following set up: a high speed, low torque prime mover followed by a gear box, and ending in a low speed, high torque output. The forward moving power path has lower efficiency losses than the backwards moving power path. That is, it is difficult for the output of the gear box to drive the input. It becomes more difficult as the gear ratio increases, i.e. smaller driving pinion and/or large driven gear [12]. This is seen in the velocity amplification map, where a large gear is driving a smaller gear. And, as the smaller gear decreases in pitch diameter, the losses of driving this system increases.

Overall, the efficiency loss of the velocity amplifier is greater than that of the torque amplifier. This is seen by the reference plane placed at 0.5% efficiency loss.

6.2 Simple Approximation of Sliding Loss for Helical Gear from Spur Equation

Very little literature exists for simple formulations of helical gear sliding losses. Generally, helical gears will have a sliding velocity increase as well as a normal force of contact $F_{c,h}$ increase relative to simple spur gears. These two increases will both increase the losses in helical gears. Hence:

$$F_{c,h} = \frac{F_{c,s}}{\cos \beta} \quad Eq. 6.6$$

where $F_{c,s}$ is the normal contact force for spur gears and β is the helical angle. Then, the sliding length L_h for helical is larger than it is for spur gears. Given that L_s is the width of a spur gear, then:

$$L_h = \frac{L_s}{\cos \beta} \quad Eq. 6.7$$

It, then, appears that the losses of spur gears l_s would be increased to give the helical losses l_h as:

$$l_h = \frac{l_s}{\cos^2 \beta} = C_1 l_s \quad Eq. 6.8$$

where C_1 is the scale factor $1 / \cos^2 \beta$. Then, Figure 6-1 and 6-2 can be scaled as follows per helical angle:

Table 6.1: Scale Factors for Helical Gears Approximate Efficiency Loss due to Sliding

β	Δl_h	C_1
0°	0	1
5°	0.01	1.01
15°	0.07	1.07
30°	0.33	1.33

Where Δl_h is the loss increase of efficiency. Note that at helical angle β of 0° the loss increase is zero because it is a spur gear.

Figure 6-1: Torque Amplifier Percent Efficiency Loss, 20° and 25° Pressure Angle, $f = 0.05$

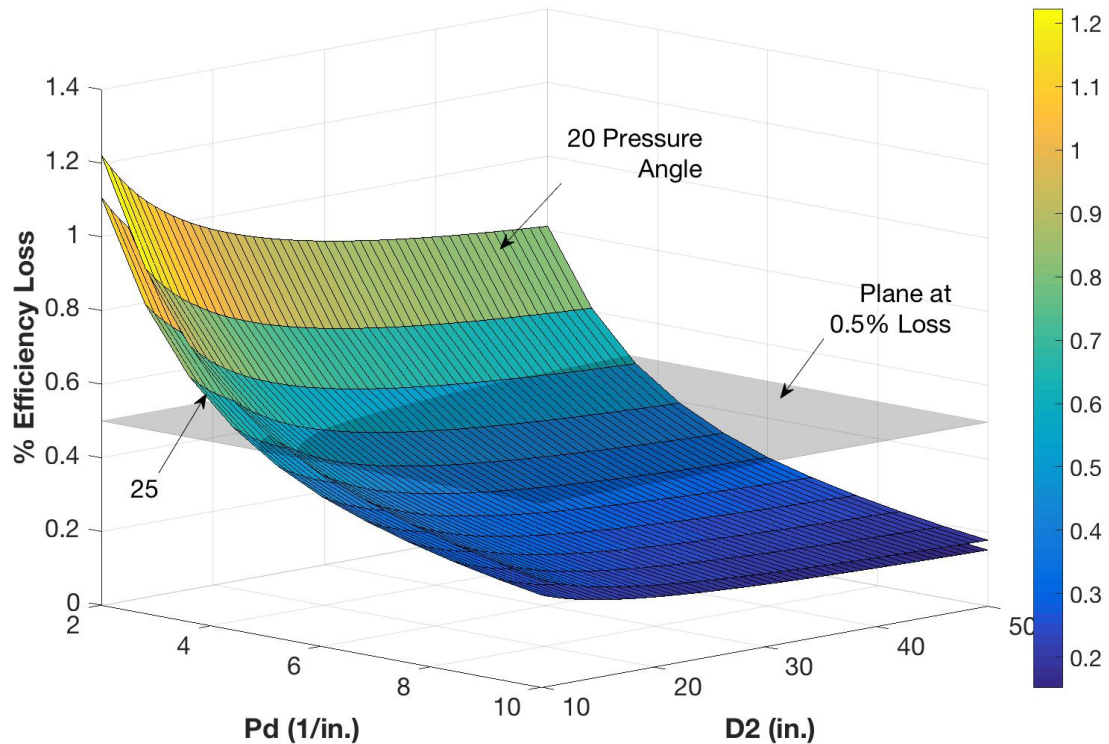
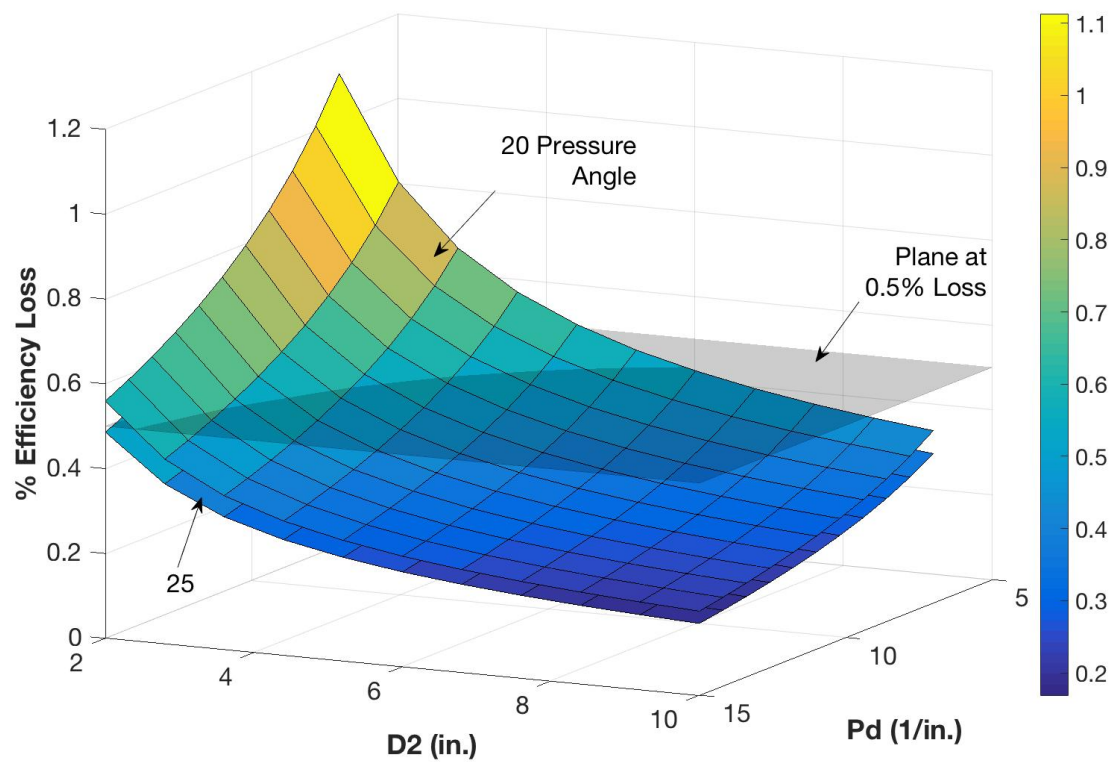


Figure 6-2: Velocity Amplifier Percent Efficiency Loss, 20° and 25° Pressure Angle, $f = 0.05$



Appendices

Appendix A1: Involute Function and the Inverse of the Involute Function

The involute function is defined as:

$$\varepsilon = \text{inv}\phi = \tan\phi - \phi$$

where ϕ is any angle.

The inverse involute function ($\phi = \text{inv}^{-1}\varepsilon$) cannot be found explicitly using elementary functions of ε , but Cheng H. [source_Cheng] presents expressions for ϕ which are derived using perturbation techniques. One of them is as follows:

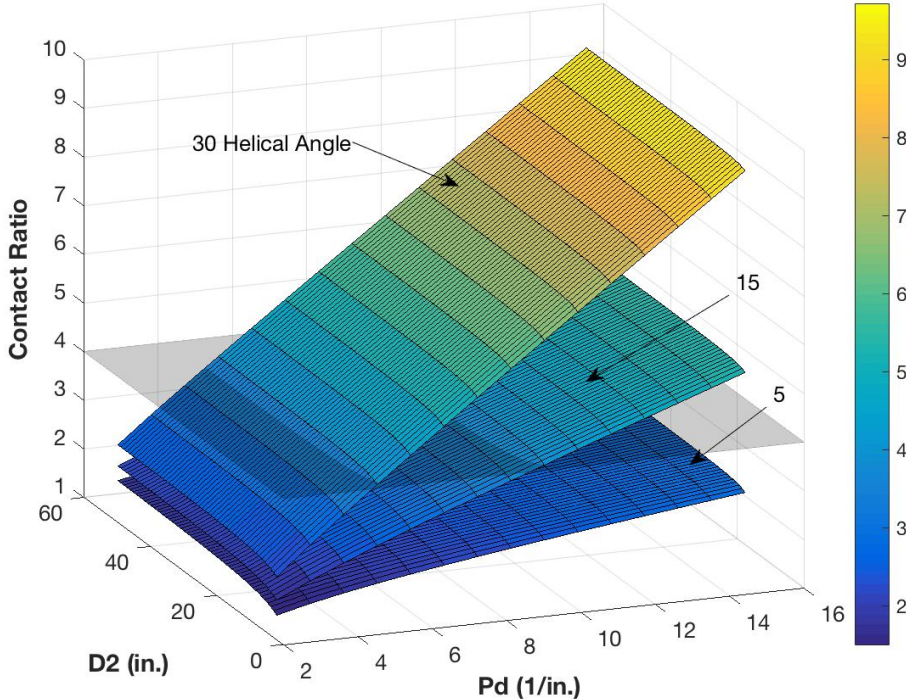
$$\phi = \text{inv}^{-1}\varepsilon \approx 3^{1/3}\varepsilon^{1/3} - \frac{2}{5}\varepsilon + \frac{9}{175}3^{2/3}\varepsilon^{5/3} - \frac{2}{175}3^{1/3}\varepsilon^{7/3}$$

This expression is only the first four terms of a longer expression containing nine terms. These four terms as is only give an error of less than 0.0018% (1.41×10^{-5} radians) when working with angles that are 45° or less, which is the case in this document [source_Cheng].

To reduce computational time, and given the small error, this expression with its first four terms will be used.

Appendix A2: Showing that Diametral Pitch and Large Teeth Count V. Contact Ratio Maps show Inconsequential Results for Spur Gears

Figure A2-1: 20° Pressure Angle, Face Width 3", Helical Angle 5° , 15° , 30°



Appendix B: Calculation of I and J Average

For this document, the I and J values are not calculated for every mesh being tested. Instead, and average is taken at every combination of pressure and helical angle. The values used to take these averages come from [source_AGMA].

For example, for the 20° pressure angle with 0° helical angle the data shown in Table B.1 is used. Based on the parameters set in Section 1, the number of teeth is bounded by the red boxes in Table B.1. The average is taken from these values.

Table B.1: I and J Factors for 20° Pressure Angle and 0° Helical Angle [source_AGMA]

I AND J FACTORS FOR:¹

20.0 DEG. PRESSURE ANGLE
 0.0 DEG. HELIX ANGLE
 0.250 TOOL EDGE RADIUS
 EQUAL ADDENDUM ($x_1 = x_2 = 0$)

2.250 WHOLE DEPTH FACTOR
 0.024 TOOTH THINNING FOR BACKLASH
 LOADED AT TIP

GEAR TEETH	PINION TEETH															
	12		14		17		21		26		35		55		135	
TEETH	P	G	P	G	P	G	P	G	P	G	P	G	P	G	P	G
12 I																
J	U	U														
14 I																
J	U	U	U	U	U	U	U	U	U	U	U	U	U	U	U	U
17 I																
J	U	U	U	U	U	U	U	U	U	U	U	U	U	U	U	U
21 I																
J	U	U	U	U	U	U	U	U	U	U	U	U	U	U	U	U
26 I																
J	U	U	U	U	U	U	U	U	U	U	U	U	U	U	U	U
35 I																
J	U	U	U	U	U	U	U	U	U	U	U	U	U	U	U	U
55 I																
J	U	U	U	U	U	U	U	U	U	U	U	U	U	U	U	U
135 I																
J	U	U	U	U	U	U	U	U	U	U	U	U	U	U	U	U

Appendix C: Maps of % Efficiency Loss Due to Sliding with 0.1 and 0.01 Coefficient of Friction

The following are design maps for percent efficiency loss from Section 6. These are included here, and not in the main text, because they only show the graph being scaled about the z-axis.

Figure C-1: Torque Amplifier Percent Efficiency Loss, 20° and 25° Pressure Angle, $f = 0.01$

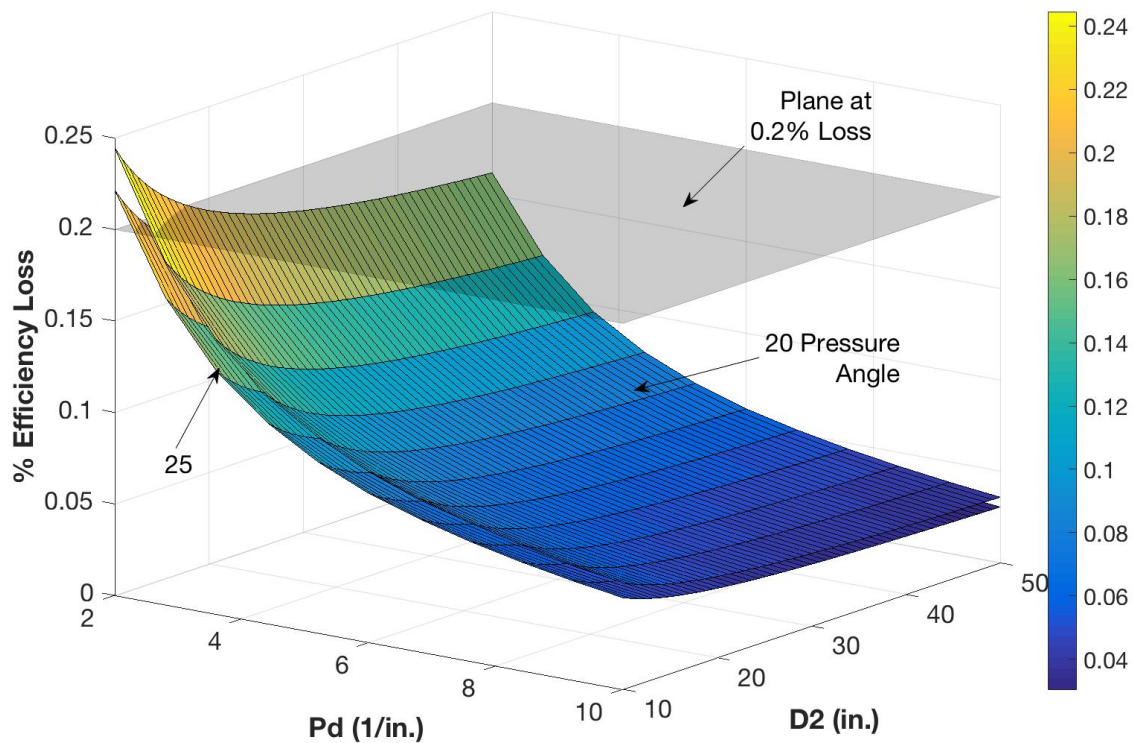


Figure C-2: Velocity Amplifier Percent Efficiency Loss, 20° and 25° Pressure Angle, $f = 0.01$

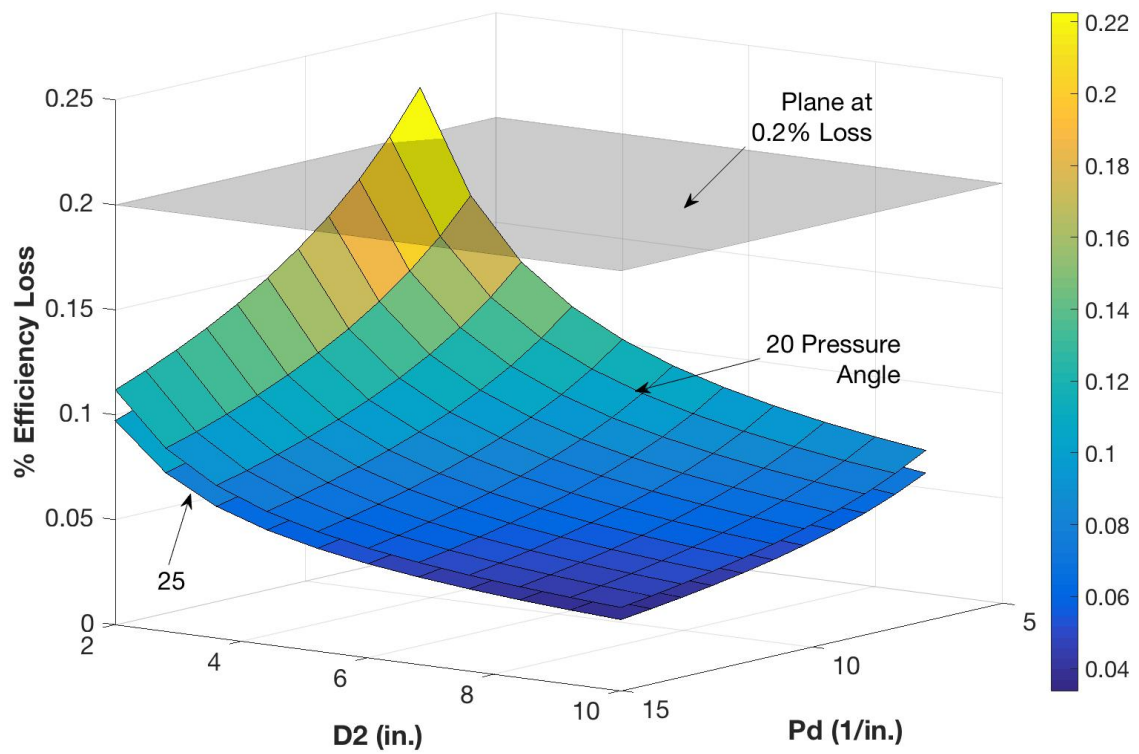


Figure C-3: Torque Amplifier Percent Efficiency Loss, 20° and 25° Pressure Angle, $f = 0.10$

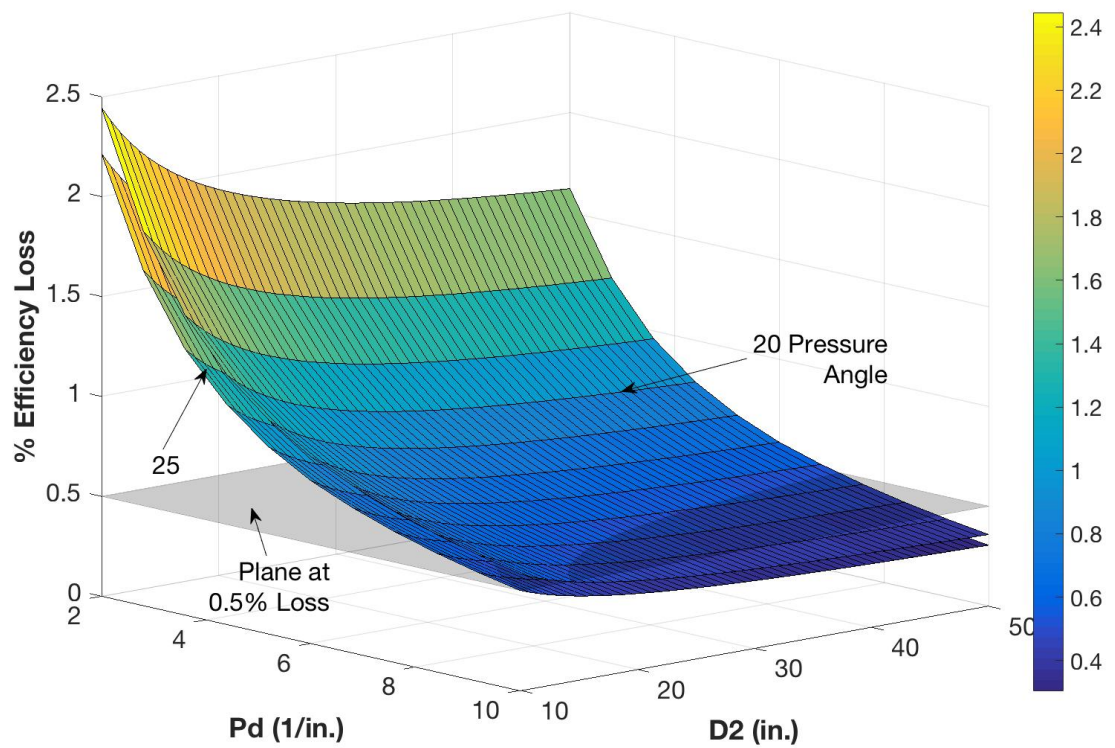
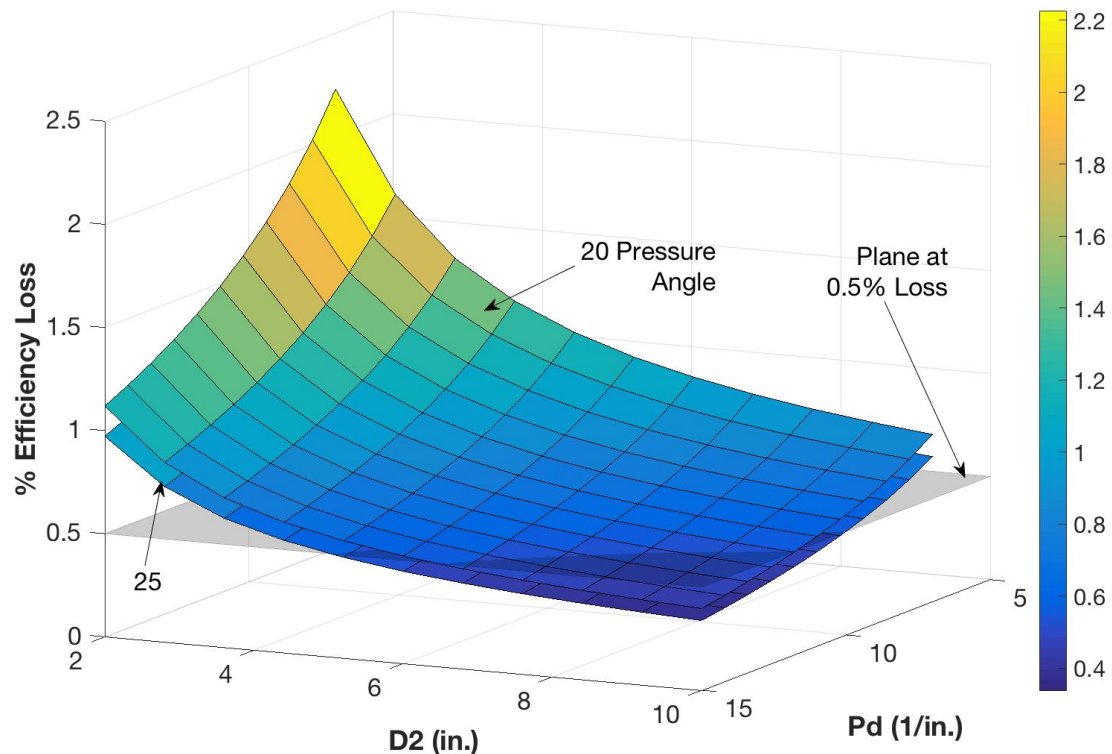


Figure C-4: Velocity Amplifier Percent Efficiency Loss, 20° and 25° Pressure Angle, $f = 0.10$



Appendix D: Friction Torque Increase Δ_1 and Δ_2 for Spur Gears

In general, the physical measure is the increase in torque at the input due to friction ($\mu = 0.01, 0.05, 0.1$) in the tooth mesh. Δ_1 measures that increase ΔT , while the output torque T_2 is also reduced (ΔT_2 can actually go to zero when the system locks up if μ is too high). The gear design objective is to maintain the output torque T_2 such that $\Delta T_2 = 0$. Which then results in an increase in input torque $\Delta_2 = \Delta T_1$. The plots shown here give the results for both Δ_1 and Δ_2 . Note that all charts are proportional to the value of μ . In general, the velocity amplification results in a Δ_2 which is about 1.6x higher than torque amplification because of the increase in the friction force moment arm.

Figure D-1: Delta 1 for 20° Pressure Angle, Velocity Amplification

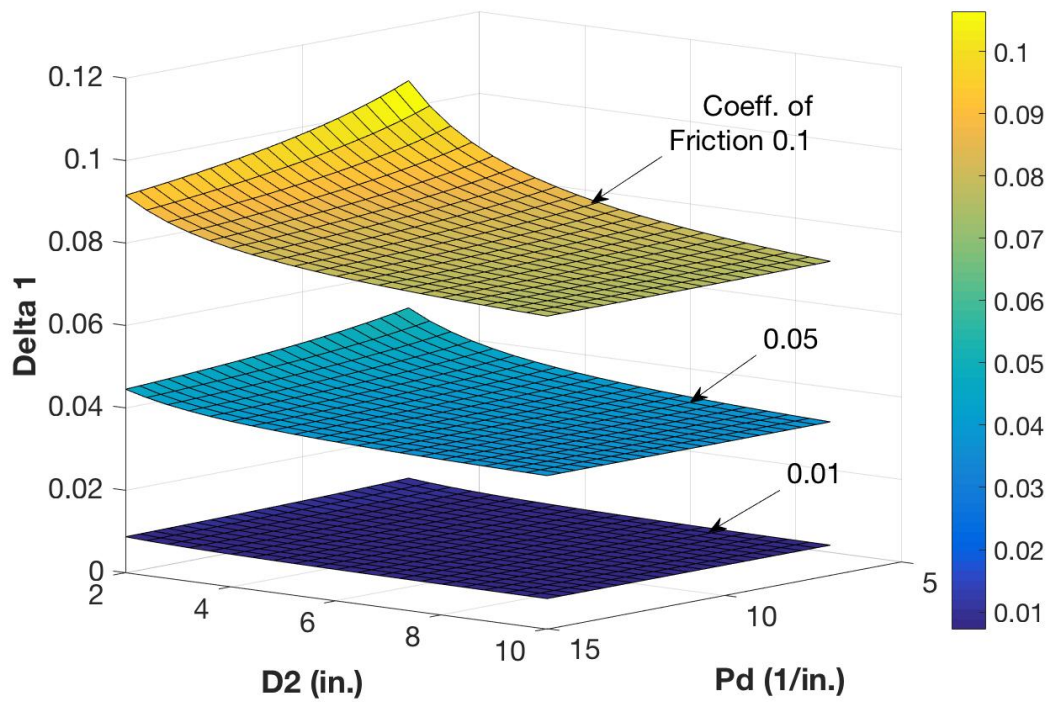


Figure D-2: Delta 1 for 20° Pressure Angle, Torque Amplification

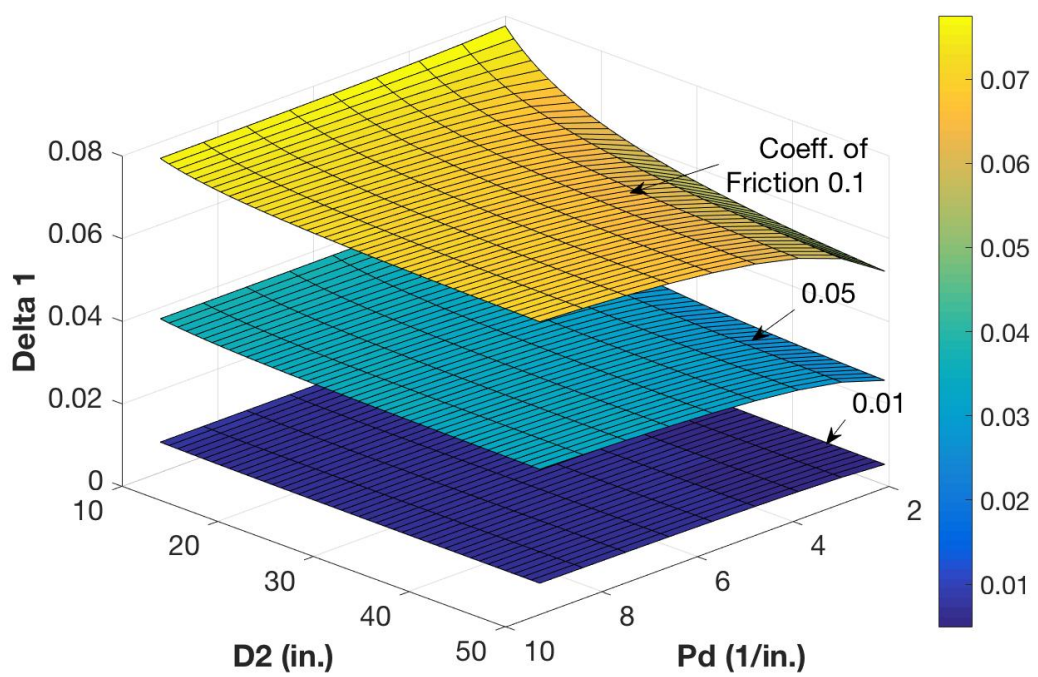


Figure D-3: Delta 1 for 25° Pressure Angle, Velocity Amplification

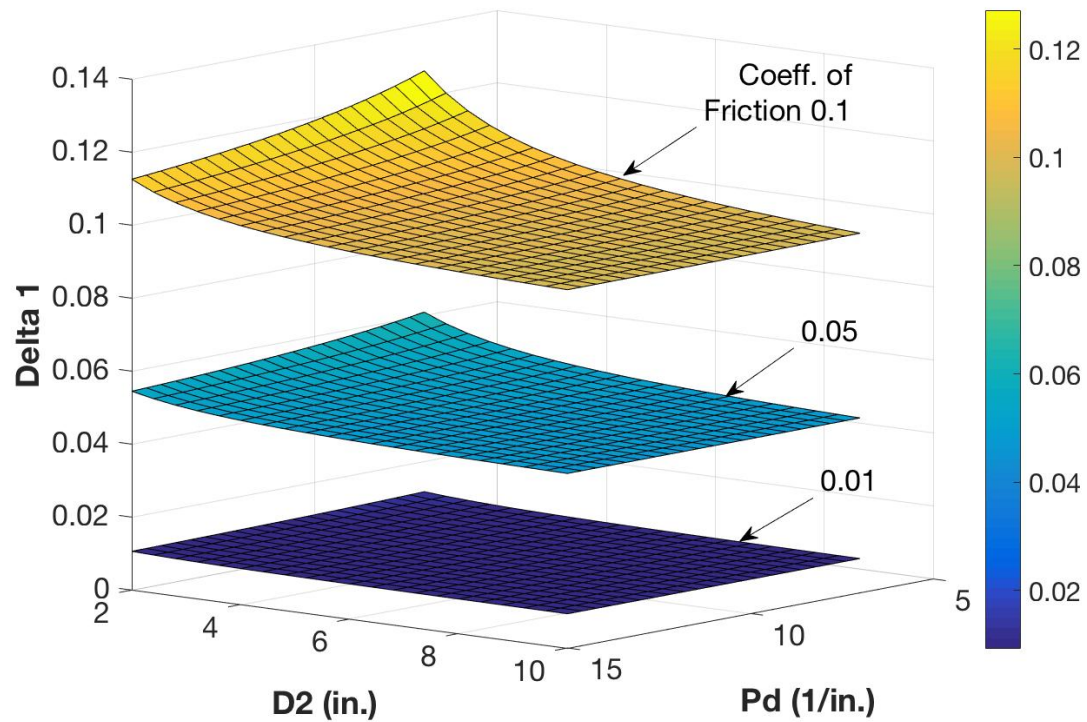


Figure D-4: Delta 1 for 25° Pressure Angle, Torque Amplification

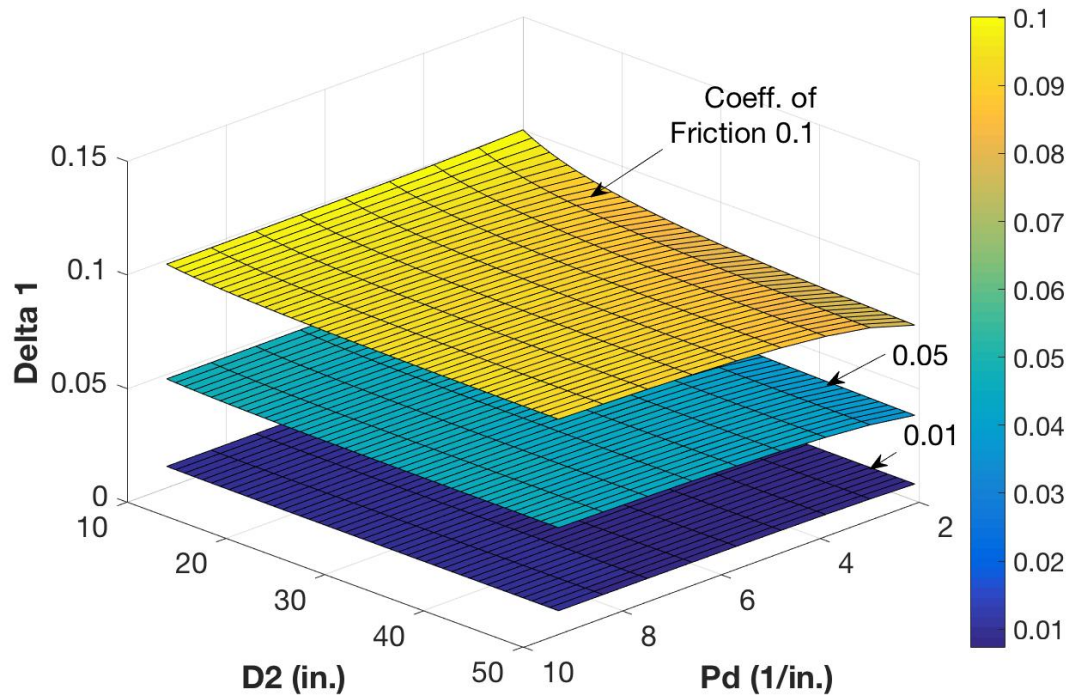


Figure D-5: Delta 2 for 20° Pressure Angle, Velocity Amplification

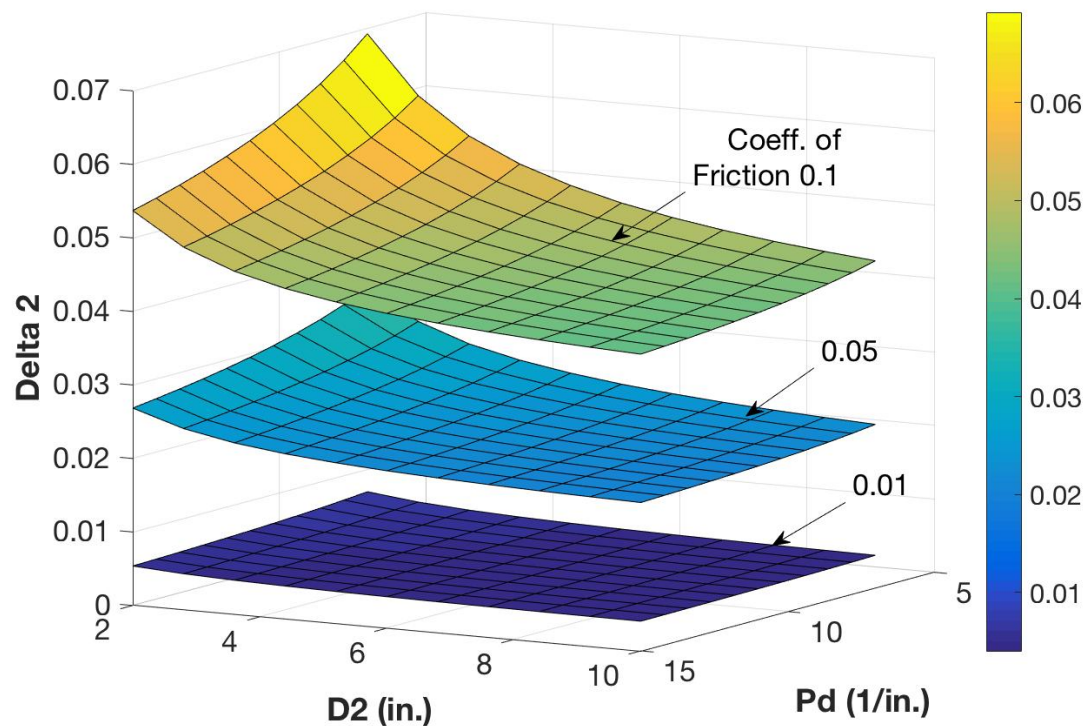


Figure D-6: Delta 2 for 20° Pressure Angle, Torque Amplification

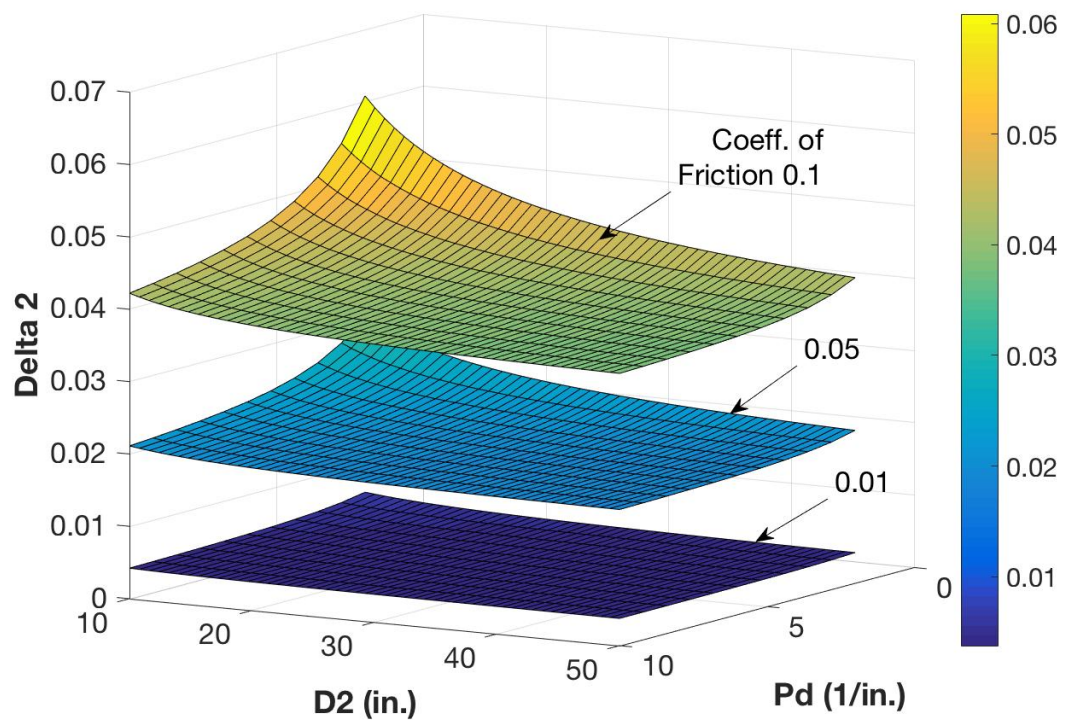


Figure D-7: Delta 2 for 25° Pressure Angle, Velocity Amplification

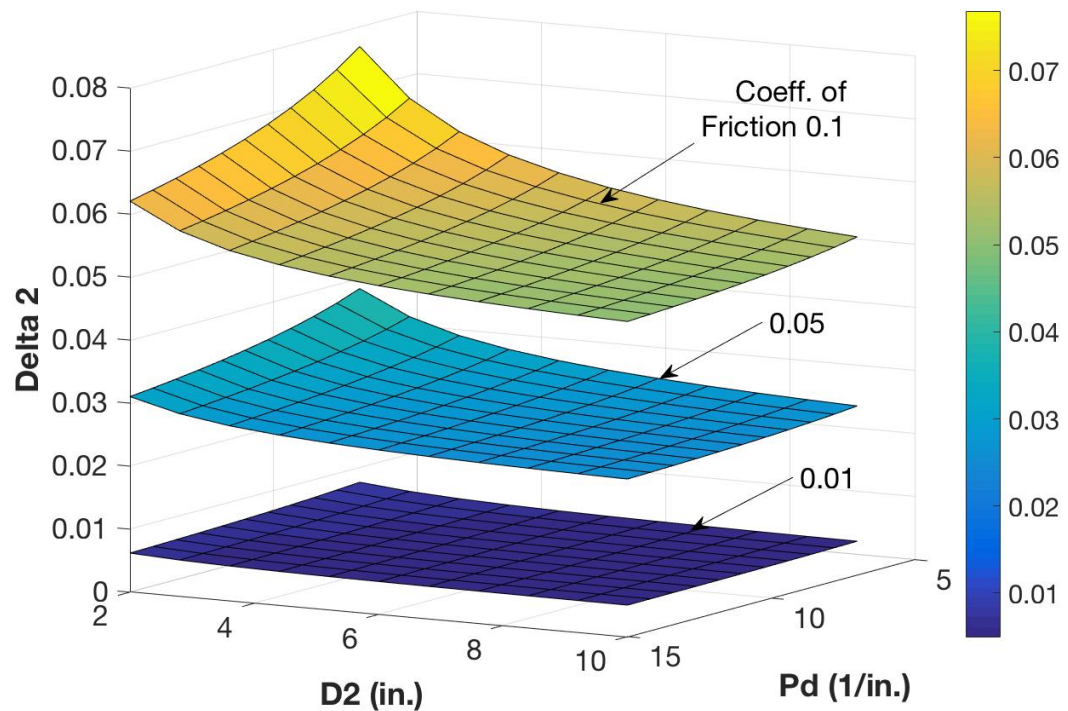
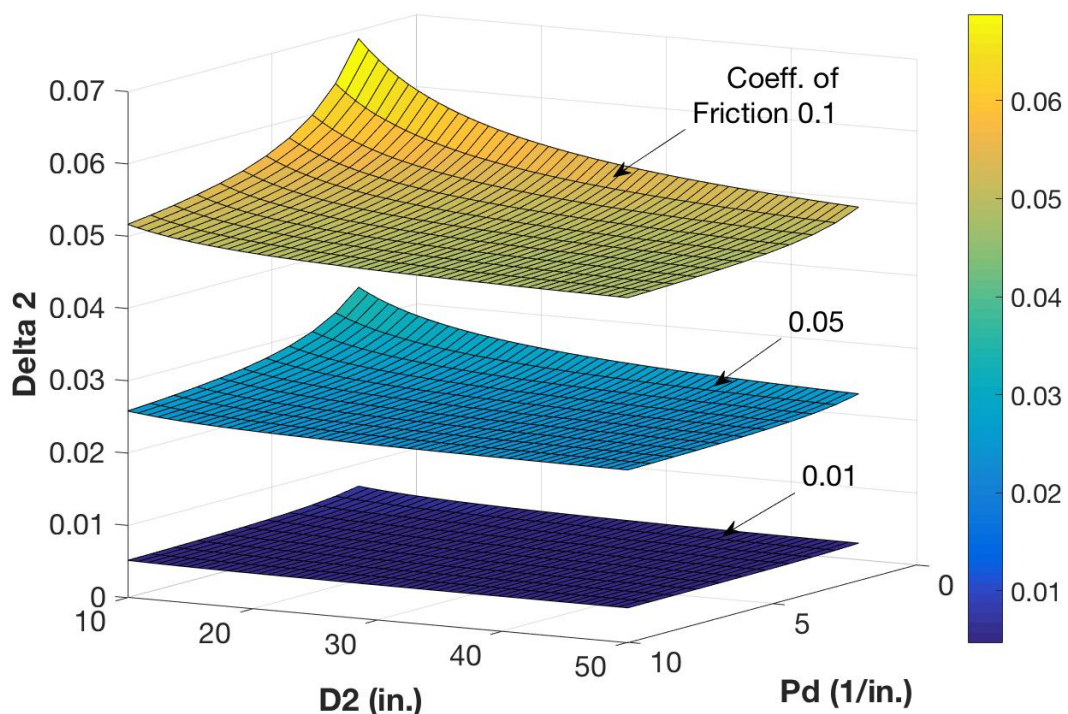


Figure D-8: Delta 2 for 25° Pressure Angle, Torque Amplification



References

- [1] Anderson, N. E., & Loewenthal, S. H. (1983). Comparison Of Spur Gear Efficiency Prediction Methods. Conference Paper. NASA.
- [2] Cheng, H. H. (1996). Derivation of the Explicit Solution of the Inverse Involute Function and its Applications in Gear Tooth Geometry Calculations. *Journal of Applied Mechanisms and Robotics*, 3(2), 13-23. Retrieved September 4, 2017, from http://iel.ucdavis.edu/publication/journal/gear_toabcoth_geometry.pdf
- [3] Collins, J. A. (2010). Mechanical design of machine elements and machines: a failure prevention perspective (2nd ed.). New York: John Wiley & Sons.
- [4] Elements of Metric Gear Technology (Tech.). (n.d.). Retrieved September 4, 2017, from QTC website: http://qtcgears.com/tools/catalogs/PDF_Q420/Tech.pdf
- [5] Kiekbusch, T., & Howard, I. (2007, December 12). A Common Formula for the Combined Torsional Mesh Stiffness of Spur Gears. In Uq.edu.au.
- [6] Klebanov, B. M., Barlam, D. M., & Nystrom, F. E. (2008). Machine elements: Life and design . Boca Raton, FL: CRC.
- [7] Materials Data Book. (2003 edition). Cambridge University Engineering Department.
- [8] Pedersen, N. L., & Jørgensen, M. F. (2014). On gear tooth stiffness evaluation. *Computers & Structures*, 135, 109-117. doi:10.1016/j.compstruc.2014.01.023
- [9] Quinones, A., Goytisolo, R., Moya, J., & Ocampo, R. (2005). Infuence of the Friction Force, the Tooth Correction Coefficient and the Normal Force Radial Component in the Form Factor and the Stress in the Feet of Spur Gear's Teeth. ASME Design Engineering, Parts A and B. doi:10.1115/imece2005-80421
- [10] Sánchez, M. B., Pleguezuelos, M., & Pedrero, J. I. (2017). Approximate equations for the meshing stiffness and the load sharing ratio of spur gears including hertzian effects. *Mechanism and Machine Theory*, 109, 231-249. doi:10.1016/j.mechmachtheory.2016.11.014
- [11] Titus, A. W. (1965). Analysis of Friction Torque in Simple and Preloaded Spur Gear Trains. NRL Report.
- [12] Wang, A., & Kim, S. (2015). Directional efficiency in geared transmissions: Characterization of backdrivability towards improved proprioceptive control. 2015 IEEE International Conference on Robotics and Automation (ICRA). doi:10.1109/icra.2015.7139307
- [13] Liu, L., & Pines, D. J. (2002). The Influence of Gear Design Parameters on Gear Tooth Damage Detection Sensitivity. *Journal of Mechanical Design*, 124(4), 794. doi:10.1115/1.1519275
- [14] Budynas, R. G., Nisbett, J. K., & Shigley, J. E. (2015). Shigley's mechanical engineering design (10th ed.). New York, NY: McGraw-Hill Education.
- [15] Lynwander, P. (1983). Gear Drive Systems: Design and Application. New York, NY: Marcel Dekker.
- [16] AGMA-908-B89. (1989). 20-52.